THERMAL MODELLING OF HIGH SPEED MACHINE TOOL SPINDLES

By:

TURGUT KÖKSAL YALÇIN

Submitted to the Graduate School of Engineering and Natural Sciences in partial fulfillment of the requirements for the degree of

Master of Science

Sabanci University

2015

THERMAL MODELLING OF HIGH SPEED MACHINE TOOL SPINDLES

APPROVED BY:

Prof. Erhan BUDAK   ....

(Thesis Advisor)

Assoc. Prof. Mustafa BAKKAL   ....

Assoc. Prof. Bahattin KOÇ   ....

Date of Approval:

To my family

TERMAL MODELLING OF HIGH SPEED MACHINE TOOL SPINDLES

Turgut Köksal Yalçın

Industrial Engineering, MS Thesis, 2015

Thesis Supervisor: Prof. Dr. Erhan Budak

Abstract

Machining is the most widely used manufacturing method by far since its foundation and its development process still continues parallel to the technology. Demand for higher quality parts together with the lower machining time and cost is rapidly increasing. In order to meet this increasing demand, high speed machining processes and equipment are getting much more important compared to the traditional methods. High speed machine tools are the key elements of this new machining era; but making the machine tools faster while improving their overall performance requires high end technology together with advanced engineering applications. Positioning accuracy of a high speed machine tool is the most important metric among others because of its direct effect on the finished parts, which are measured as dimensional errors. The highly strong and nonlinear relationship between the positional accuracy and the thermal characteristics of the machine tools raises the importance of modeling the thermal behavior of the machine tools.

The main aim of this thesis is to develop robust thermal models for high speed machine tool spindles, by considering the effects of built-in cooling systems, to be able to predict and then reduce the positioning errors related to the thermal behavior of the spindle unit. Fully analytical approaches are very complex for solving the nonlinear thermal behavior of the spindle units; but they are still powerful when they used together with the finite elements model of the complex spindle geometry. As the first step of the thermal model, the heat generated by the ball bearings, which is considered as the main heat source of the entire spindle unit, is calculated analytically. Calculated

heat is used as an input to the Finite Elements Method (FEM) model for the heat transfer and thermal error calculations. Built-in cooling system of the spindle unit is also analyzed using the Computational Fluid Dynamics (CFD) approaches again using FEM models. Overall temperature distributions and thermal elongations leading to positioning errors are calculated by the FEM model. Simulation results are validated by temperature and thermal elongation experiments measured on a 5-axis CNC machine tool spindle. Cooling system parameters optimization is achieved by using the developed models as quick solutions to the positioning problems. On the other hand cooling system design improvements are also analyzed by the developed models and several different cooling channel designs are investigated for increasing the positioning accuracy of the high speed machine tool spindle used in the experiments. Overall good agreement is observed between experiments and simulations.

YÜKSEK HIZLI İŞ MİLLERİNİN TERMAL MODELLENMESİ

Turgut Köksal Yalçın

Endüstri Mühendisliği, Yüksek Lisans Tezi, 2015

Tez Danışmanı: Prof. Dr. Erhan Budak

Anahtar Kelimeler: Yüksek Hızlı İş Mili, İş Mili Termal Uzaması, Termal Hata Modellemesi, Sonlu Elemanlar Analizi, Soğutma Sistemi Analizi

Özet

Talaşlı imalat, bulunuşundan bu yana en çok tercih edilen imalat yöntemlerinin başında gelmekte ve ilerleyen teknoloji ile paralel olarak gelişimini sürdürmektedir. Daha hassas toleranslara sahip parçaların daha hızlı, daha kaliteli ve daha ucuza üretilmesi yönündeki talep gün geçtikçe artmaktadır. Artan bu talebin karşılanabilmesi için geleneksel yöntemlere nazaran yüksek hızlı işleme yöntemleri ve ekipmanları daha da önem kazanmaktadır. Talaşlı imalatın yeni döneminin kilit elemanları olan yüksek hızlı takım tezgâhları, işleme hızı ile birlikte genel performans artışı sağlayabilmek adına en son teknolojiler ve yenilikçi mühendislik uygulamaları kullanılarak geliştirilmektedir. Geleneksel takım tezgâhlarında olduğu gibi yüksek hızlı tezgâhlarda da pozisyonlama hassasiyeti son parça boyutlarına doğrudan yansıdığı ve boyutsal hatalar doğurduğu için tezgâh değerlendirme kriterleri arasındaki en önemli faktördür. Pozisyonlama hassasiyetinin tezgâhların termal karakteristikleri ile son derece kuvvetli ve karmaşık ilişkisi, yüksek hızlı takım tezgâhlarındaki termal davranışların modellenmesinin önemini arttırmaktadır.

Bu tez çalışmasının amacı, yüksek hızlı iş millerinde sıcaklığa bağlı oluşan pozisyonlama hatalarının doğru tahmin edilebilmesi ve azaltılabilmesi için iş mili üzerindeki dahili soğutma sistemi etkilerini de göz önünde bulunduran termal modellerin oluşturulmasıdır. Zamana bağlı ve lineer olmayan sıcaklık denklemlerinin kompleks geometriler ile birlikte tamamen analitik yöntemlerle çözümü son derece zor olduğundan; sonlu elemanlar yöntemine baş vurulmuştur. İş mili sıcaklık kaynaklarının en önemlisi olan iş mili bilyalı yataklarının ürettiği ısı miktarı analitik olarak hesaplanması modelin ilk adımıdır. Hesaplanan ısılar iş mili sonlu elemanlar modeline(SEM) aktarılarak iş mili elemanları arasındaki ısı transferleri ve bu transferler

sonucu oluşan termal uzamalar hesaplanmıştır. İş milinde bulunan dahili soğutma sistemi, akışkanlar dinamiği çözümleri için yine sonlu elemanlar analizi kullanılarak incelenmiştir. Isı kaynakları ve soğutma sistemleri sonucu oluşan sıcaklık dağılımları ve termal uzamalardan kaynaklanan pozisyonlama hataları SEM kullanılarak hesaplanmıştır. Oluşturulan modele ait simülasyon sonuçları 5 eksenli CNC takım tezgahı üzerinde yapılan sıcaklık ve termal uzama testleri ile doğrulanmıştır. Pozisyonlama hatalarına pratik bir çözüm olarak soğutma sistemine ait parametrelerin iyileştirilmesi yine oluşturulan modeller üzerinden yapılmıştır. Soğutma sistemi dizayn iyileştirmesi yönünde farklı kanal geometrilerinin iş mili sıcaklık dağılımına ve pozisyonlama hatalarına olan etkileri simülasyonlar aracılığı ile incelenmiştir. Simülasyon ve test sonuçlarının birbirine yakın olduğu gözlenmiştir.

ACKNOWLEDGEMENTS

LIST OF FIGURES

LIST OF TABLES

CHAPTER 2

2. INTRODUCTION

2.1 Introduction and Literature Survey

Machining is still the most commonly used manufacturing method for high accuracy- critical to operation parts of the aerospace and defense industries; even though it is one of the oldest methods. Machining technology is continuously developing with the new requirements and demands of these two industries. New materials, design methodologies and treatments are tightening the part quality specifications so that machine tool technologies need continuous updates in order to meet these specifications. CNC machine tool manufacturers are trying to optimize their products by changing mechanical designs, materials used for the components, outsourced components and control algorithms. Overall performance of a machine tool can only be improved if all the contributors to the machine tool error term are improved together. Positioning accuracy on the other hand is one of the most important aspects of a CNC machine tool due to its direct effect on the finished parts. Major factors affecting the machining and positioning accuracies of the machine tools are:

- Cutting forces generated by the cutting tool,
- Nonlinear heat, generated by both the cutting operation and electrical components throughout the machine tool running time,
- Inaccuracies of the components due to manufacturing and assembling stages,
- Environmental temperature and heat sources,
- Errors due to the control system of the machine tool.

Among all these important factors, heat generation and the geometrical errors related to this generated heat are responsible up to %75 of the total machine tool errors [1]. Heat

generation mechanism of the machine tools are complicated due to the time dependency and non-linear behavior of the heat sources that contribute to the overall heat generation; such as axis motors, linear guideways, ball screws, spindle motor and bearings. Fully analytical computation of the heat generated in these sources is so hard that mathematical models are developed for estimating the heat values. Estimating the heat generated by all these components is still not enough to calculate the overall temperature distribution and thermal deformations, because of the complicated machine tool designs that are composed of different components and sub systems. The crucial effects of thermal errors are fully recognized after the inaccuracies due to the mechanical design and assembling technologies are minimized by the developed technology in machine tool industry. Researchers found that eliminating only the physical errors in machine tools is enough to produce parts with tighter tolerances.

Bryan is well known by his studies about thermal effects in both machine tool technologies and metrology between 1963 and 1985. He published several papers about the thermal effects in dimensional measurements [2], cutting tool thermal elongations while chip removal [3] and machine tool spindle growth due to temperature rise [4]. Most of these primary studies are based on measuring temperature changes together with dimensional measurements of tools or devices in order to link both results. Thermal error studies of the machine tools mainly focused on the compensation of the thermally induced errors. Zhang et al [5] studied error compensation techniques for the coordinate measuring machines; he used rigid body kinematics and quick axis measurements to compensate positioning errors of the CMMs first, then applied same methodology to the machine tools. Weck [6,7] presented several direct and indirect compensation methods starting with lathes and then for the machine tools in general. He used the simple inputs such as motor currents, spindle speeds and environmental speeds to estimate the thermally induced errors. Dönmez et al. [8] also worked on error compensation for both measuring machines and machine tools; he used 3 step feature based measurement technique to identify error mechanisms. Moriwaki et al. [9] focused on the thermally induced errors of the spindle units specifically. He investigated the effect of the environmental temperature on the spindle thermal errors for the ultra-precision air spindle systems.

Thermal performances of the machine tools are investigated component vise due to the high number of components which are contributing the overall heat generation. The

most important component of a machine tool for thermal behavior is the spindle unit. High speed rotational movement used for chip removal is generated at the spindle unit and due to frictional losses during this generation of the rotational movement heat is generated [10]. Main contributors of the generated heat in the machine tool spindles are:

- Spindle bearings
- Spindle motor
- Cutting operation

Modelling of the machine tool temperatures was always being a hot topic for the researchers. Several approaches are used for the thermal performance studies, such as analytical modeling techniques; which are developed to estimate the amount of heat generated during the process using mathematical equations and physical theories; and mapping techniques; which are used to create meaningful linkages between the measured temperatures and measured thermal deformations. Most of the early studies are categorized as mapping techniques. Some of the popular approaches used in these kinds of studies are multiple-linear regression methods, artificial neural networks, grey system theory, fuzzy logic systems. Regression analysis is still used in the recent studies; Chen et al. [11] used basic linear regression analyses to compensate for the thermally induced errors of a double column machining center. Wang et al. [12] used the regression method to estimate thermal growth of the precision cutter grinders. He established a compensation map by interpolating the results of several experiments by regression method. Li et al. [13] developed a thermal compensation algorithm using auto-regressive models so that he could directly calculate the compensation coefficients from the NC code generated to manufacture parts. Artificial neural networks are used very often for mapping the temperature and deflection measurements. By constructing a smart training data, which contains possible scenarios and inputs to the systems, these methods can estimate the outputs of a system to an unknown input successfully. Hattori et al.[14] constructed a three layer feed forward neural net structure to estimate the relationship between environmental temperatures and thermal displacements of a vertical milling tool. Vanherck et al. [15] used artificial neural network with a single layer 4-neuron model to estimate and compensate thermally induced errors of a 5-axis milling machine. He reduced the maximum deformations of the tool tip from 150μm to 15μm with the proposed method. Mize and John [16] applied neural networks based

modelling approach together with kinematic error measurement method to a 3-axis machine tool concluding in a 7μm of three dimensional positioning accuracy.

Analytical modeling techniques are for spindle thermal performance is studied by many researchers; main aim of these studies is to predict thermally induced errors by mathematical calculations and theories beforehand in order to compensate them. For the analytical modeling techniques, spindle bearings are the most studied sources of thermal performance researches. First and still widely used analytical method for predicting the spindle temperatures was found by Palmgren [17]. He used rolling friction theory to model the heat generation mechanism in spindle bearings and assumed that the bearings are the only heat sources in the system. Rolling friction theory presented by Palmgren was developed by Harris [18]; gyroscopic moments of the bearing balls are added to the system. He also worked on bearing stability and provided a handbook for proper bearing selection together with bearing life-time estimations. First one dimensional heat transfer of the Palmgren's bearing heat equations are presented by Burton and Staph [19]. Jorgensen [20] constructed a quasi-three dimensional heat transfer network for spindle temperature analysis by considering the bearings and motor as the main heat sources. Stein and Tu [21], by combining the bearing heat model developed by Harris with a more complex analytical heat transfer equations, they calculated the temperature distribution of a spindle unit. By the addition of heat generated in spindle motor, Bossmanns and Tu [22, 23] presented a new power flow model for estimating the spindle temperature distribution. Another study based on the heat generation at the spindle bearings was done by Li and Shin [24]; they investigated the effects of bearing configurations on both thermal and dynamical aspects of the spindle units. Mostly used bearing configurations are studied and compared according to the results of the thermo-mechanical model presented in the paper. Thermo-mechanical models for bearings are also developed by Li and Shin [25, 26] using the finite element approaches. Spindle shaft, motor and bearings are divided in small elements for calculations of dynamical behavior and thermal interactions. Conduction of heat from motor and bearings are calculated iteratively by following the finite elements method. Thermal expansions of the individual components are estimated. Min et al. [27] presented a detailed thermal model especially for spindle bearings by using the initial approaches of Bossmanns and Tu. They included the thermal contact resistance in their calculations of the heat generation at the spindle bearings. They implemented the improved thermal model of

the previous versions on a grinding machine with a conventional spindle bearing. Thermal expansions of the overall system are also calculated using their model. Jin et al. [28] used the internal load distribution of the angular contact ball bearings to calculate the heat generation. Frictional and sliding torques within the bearing balls and raceways are added to the bearing thermal model presented by Harris [18]. Effects of the external loads on the bearing temperatures are also included in their model.

The bearing heat generation model used in this study is the one presented by Harris [18]; even though his modeling approach is empirical it is still the most widely used approach by researchers. Harris considered all types of bearings while generating his data set during 1973; including the state of the art, high speed angular contact bearings with ceramic balls inside. These ceramic ball bearings were used in the aerospace applications in that time and started to be used in the machine tool industry by the early 90s. Considering the fact that the design of the angular contact bearings haven't been changed much after their foundation, recent studies about the machine tool bearings are still using Harris's [25,27,28,37] model for heat predictions. The cooling systems and materials on the other hand are the rapidly developing technologies for the thermal problems of the machine tool industry compared to the almost mature bearing technologies.

2.2 Objective

Thermal modelling of spindle units is quite important for improving the accuracies of machine tools. In case of 5 axis high speed spindle units used in high precision manufacturing applications of aviation and defense industries, thermal issues are the main reasons of scrap parts. Constructing a thermal model for estimating the thermal deformations of the machine tools accurately is very important for both machine tool builders and machine tool users. Such models can be used by machine tool builders in the design stages to reduce the thermal dependencies by better material selection, thermally robust designing and avoiding excess heat generations. These models can also be used by machine tool users for compensating the thermal errors by predicting them beforehand. The ease of usage is a crucial parameter for industrial applications, instead of just mathematical equations or lines of codes, providing visual feedback of temperatures and deformations will be more effective for all users. Implementing such a

model based on 3D CAD data will be useful for designers to easily test the thermal performances of their prototypes leading them to optimize their designs instantly.

The objective of this thesis is to come up with an industrial methodology; which can accurately and robustly estimate the temperature distributions, heat sources, cooling systems and finally the thermally induced errors of a high speed 5 axis machine tool spindle unit; so that both machine tool builders-end users can easily use to monitor thermal performances of their machine tools and optimize their designs or strategies.

2.3 Layout of the Thesis

The organization of this thesis is as follows:

In Chapter 2, high speed spindles and geometry of the bearings used in these spindles are explained. Finite elements methods of thermal modeling together with the bearing heat generation assumptions are presented.

In Chapter 3, bearing heat generation formulas are presented with the calculated heat values for the bearings used in the spindle unit modeled. Effect of spindle speed and bearing preloads are discussed. Methodology used for the heat partitioning is explained. Heat transfer coefficients for the convection are also explained in this chapter.

In Chapter 4, FE model of the spindle unit is presented together with the solid models and inputs. Different modules of the FE software, ANSYS, are explained in detail with example results.

In Chapter 5, verification tests for the FE model are explained. Comparison of the results from FE model developed and measurements done in the laboratory are shown. Performance of the developed model for estimating the temperature distribution and thermal deformations are discussed.

In Chapter 6, optimization of the cooling system parameters and geometry based on the developed thermal model is presented. Results of these optimizations are shown and compared to the current cooling systems results.

In Chapters 7 and 8, suggestions for the further research and discussions are presented.

CHAPTER 3

3. BEARING HEAT GENERATION

3.1 Introduction

In this section the heat generated in the machine tool spindle bearings due to the rotational velocity of the spindle shaft is calculated. Bearing heat generation approaches introduced by Palmgren [17] and developed by Harris [18] are discussed. Two components of the bearing heat, friction torque due to applied load and friction torque due to lubricant viscosity are explained and calculated. The effects of bearing preloads are underlined with the new axial load definitions for the angular contact ball bearings. The effect of bearing diameter is also shown by comparing two different sized bearings heat generation which are used in the investigated spindle unit. Spindle speed is a key parameter in the heat calculation of the rotating bearings. In order to show the relationship between the spindle speed and generated heat in the bearings, simulations are done with several spindle speed values within the range of the investigated machine tool spindle. Once the heat generation is calculated, method used in this study for the distribution of total generated heat between the inner and outer rings of the individual bearings is explained. Calculations of the convective heat transfer coefficients are also shown at the end of the chapter.

3.2 Friction Torque and Heat Due to Applied Load

Friction is inevitable when ball bearings are used even if complex lubrication systems

and fluids are used. In case of the rolling bearings, the continuous friction force generated within the bearing assembly creates a friction torque in the negative direction to the rotation of the spindle shaft. This friction torque is the main reason of the energy loss in the form of heat generation for the spindle bearing systems. One of the major contributors to the friction taking place between the bearing rings and bearing balls is the load applied on the bearing as shown in Figure 3. 1.
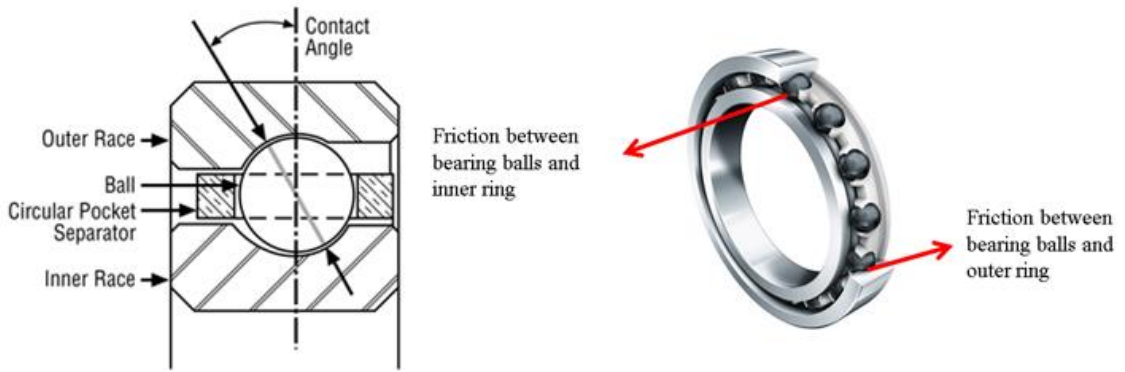
Figure 3. 1: Angular contact ball bearing (Source: Schaeffler)

This applied load is categorized into two components according to the direction; axial load F_a (N) and the radial load F_r (N). Harris [18] calculated the friction torque caused by the applied loads M_{load} (Nmm) on a bearing by the following approximation:

$$M_{load} = F_\beta f_1 d_m \tag{1}$$

Friction torque is calculated as a function of dynamical equivalent load term F_β (N) multiplied by the bearing coefficient f_1 and the average bearing diameter d_m (mm). According to the bearing manufacturers' catalogue [29] the dynamical equivalent load term is approximated using radial and axial components of the bearing loads by the following:

$$F_\beta = F_a - (0.1)F_r \tag{2}$$

In case of the vertical spindles while there is no cutting operation, the radial load acting on the spindle bearings is considered as zero resulting that the dynamical equivalent load is equal to the axial load only.

$$F_\beta = F_a \tag{3}$$

8

In this study, axial load component of an angular contact ball bearing is calculated as the combination of bearing preload values $F_{preload}$ (N) together with the gravitational force due to shaft weight $F_{gravity}$ (N). Since there is no cutting operation, cutting forces are all assumed to be zero. With this new definition of the axial load components, the effect of the bearing preload on the overall bearing heat generation is identified. The axial load of an angular contact ball bearing is calculated as the following:

$$F_a = F_{preload} + F_{gravity} \tag{4}$$

The bearing coefficient term (f_1) used in the torque calculations is a factor depends on the bearing design and bearing loads. It is calculated by the following formula:

$$f_1 = z(\frac{P_o}{C_0})^y \tag{5}$$

Parameters P_o and C_0 are the bearing dependent static equivalent load and basic static load ratings respectively, while z and y values for various bearing types are calculated by Harris [18] and given in Table 3. 1. Values of C_0 are given in the bearing catalogues, these catalogues are also giving the necessary formulas for calculating the P_o. For the bearing sets used in the investigated spindle unit, 15° angular contact ball bearings, calculations of the P_o are given in Figure 3. 2[30] in terms of axial static bearing load F_{0a} and radial static bearing load F_{0r} acting on the bearing. The average bearing diameter d_m (mm) is calculated simply by dividing the summation of inner and outer bearing ring diameters by two.

Ball Bearing Type	Nominal Contact Angle	z	y
Radial Deep Groove Bearings	0°	0.006-0.004	0.55
Angular Contact Bearings	30°-40°	0.001	0.33
Thrust Bearings	90°	0.0008	0.33
Double-Row, Self-Aligning Bearings	10°	0.0001	0.4

Table 3. 1: z and y values of different bearing types

Bearings with contact angle 15°

Load ratio	Equivalent static load
$\dfrac{F_{0a}}{F_{0r}} \leqq 1{,}09$	$P_0 = F_{0r}$
$\dfrac{F_{0a}}{F_{0r}} > 1{,}09$	$P_0 = 0{,}5 \cdot F_{0r} + 0{,}46 \cdot F_{0a}$

Figure 3. 2: Calculations of load ratio and equivalent static loads

Contact angles of the bearings are selected according to the application and loading, the only influential parameter for bearing selection is the load ration of axial to radial loads acting on the bearing. The values of the friction torque for both bearing types used in the investigated spindle assembly are calculated according to the explained procedures above by using a MATLAB code. Calculations are performed by considering different preload values in order to show the effect of the preload on the friction torque and shown in Figure 3. 3 . The two different bearing types used in the investigated spindle unit are as follows:

- FAG HC 7011: is the upper bearing with inner ring diameter of 55 mm,
- FAG HC 7014: is the lower bearing with inner ring diameter of 70 mm.
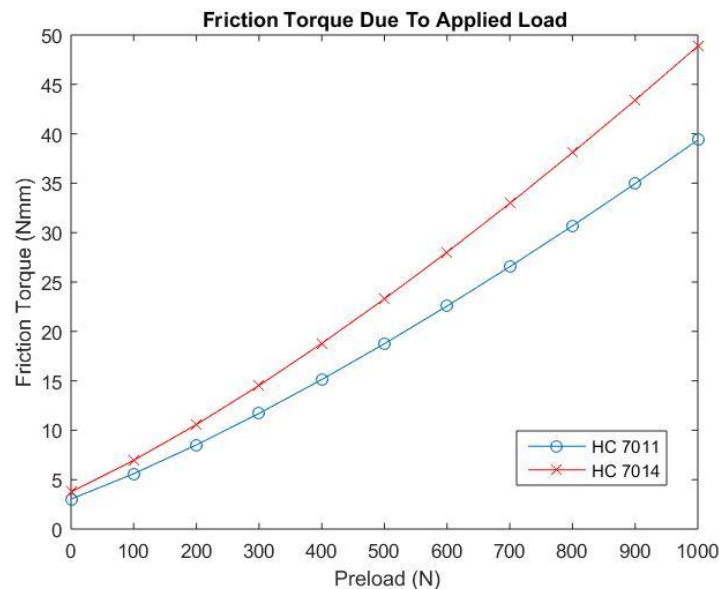
Figure 3. 3: Friction torque due to applied load

Once the frictional torques due to the applied loads are calculated, contribution of these torque values to the overall bearing heat H_{load} (W) are calculated using the spindle

speed n (rpm) by the following empirical formula presented by Harris after numerous calculations with various kinds of bearings [18] :

$$H_{load} = (1.047x10^{-4})nM_{load} \qquad (6)$$

Heat generated by the applied loads is calculated for both bearings individually, considering the effect of spindle speed and the bearing preloads. Heat generation results of the two different bearings are shown in

Figure 3. 4 and

Figure 3. 5. It can be clearly seen that the heat generation is directly proportional to preload and the spindle speed. The difference between the diameters of the bearing sets is the only reason of the difference in the calculated heat values.
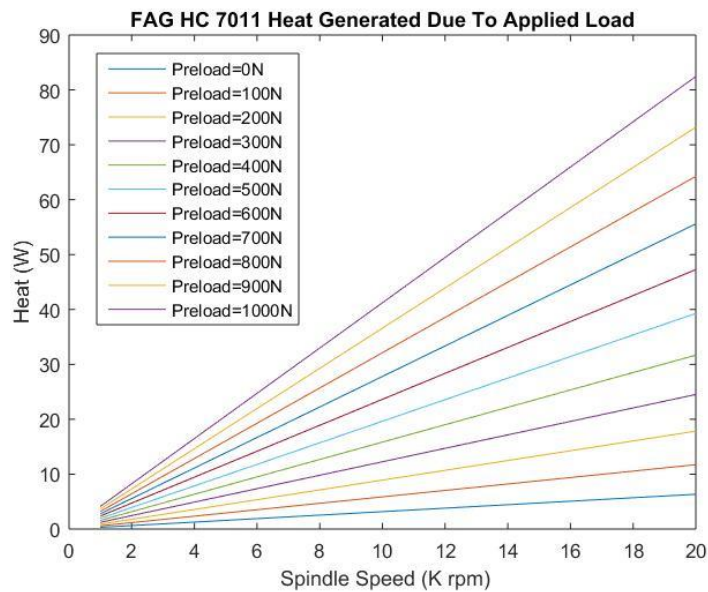
Figure 3. 4: Heat generation due to applied load 7011

3.3 Friction Torque Due to Viscosity of the Lubricant

Lubrication is vital process for increasing the fatigue lives of the mechanical joints and continuously moving parts because of its friction reducing effect. There are different kinds of lubrication systems and lubricants according to the bearing types and field of application. In case of high speed ball bearings, grease lubrication is the most widely used technique. The complexity of the bearing geometry, temperature dependent

11
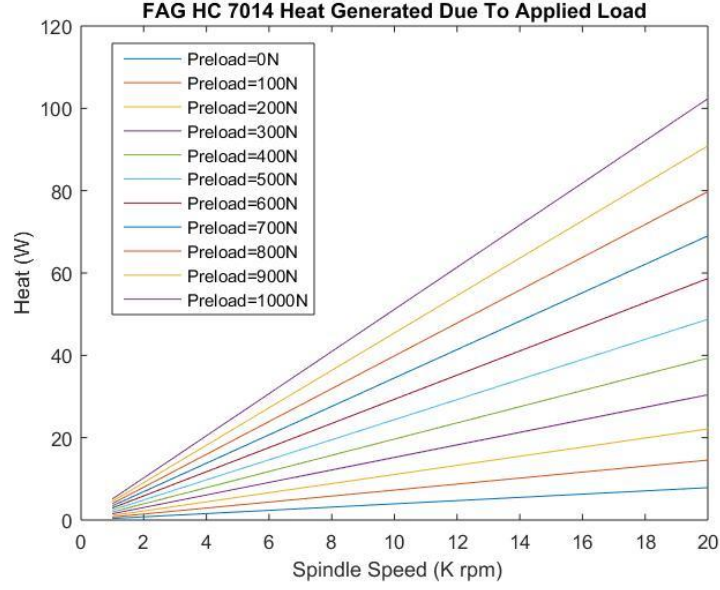
Figure 3. 5: Heat generation due to applied load 7014

material properties and time dependency make the analytical computation of the friction torque almost impossible. Palmgren [17] developed an empirical formula for the viscosity based friction torque $M_{viscous}$ (Nmm) calculations of different types of bearings as follows:

$$M_{viscous} = f_o(v_o n)^{\frac{2}{3}} d_m^3 10^{-7} \qquad if \quad v_o n \geq 2000 \qquad (7)$$

$$M_{viscous} = 160x10^{-7} f_o d_m^3 \qquad if \quad v_o n \leq 2000 \qquad (8)$$

Viscous friction torque is expressed as a function of spindle speed n (rpm), average bearing diameter d_m(mm), kinematic viscosity of the lubricant used in the bearing assembly v_o(mm^2/s) and bearing coefficient f_o. The value of f_o depends on the bearing type and lubricant, shown in Table 3. 2 below [31].

Value of f_o				
Ball Bearing Type	Grease	Oil-Mist	Oil-Bath	Oil-Jet
Deep Groove Bearings	0.7-2	1	2	3-4
Angular Contact Bearings	2	1.7	3.3	6.6
Thrust Bearings	5.5	0.8	1.5	3
Self-Aligning Bearings	1.5-2	0.7-1	1.5-2	3-4

Table 3. 2: Values of f_o for different bearing types

Kinematic viscosity of the lubricant used in the bearing systems is effective on the friction torque calculations only if higher spindle speeds are used as stated in the formula. The values of the kinematic viscosity vary with the operating temperature and are given in bearing catalogues. Calculated viscous friction torques of both bearings is shown in

Figure 3. 6.
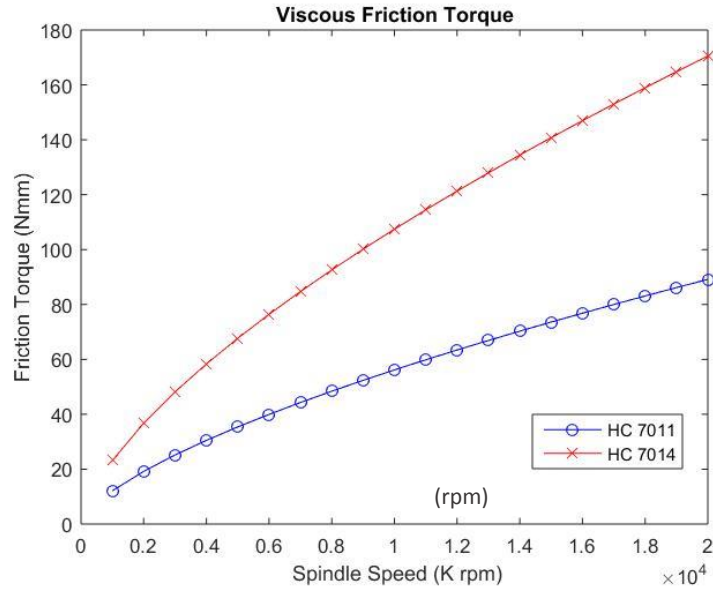
Figure 3. 6: Viscous friction torque

Conversion from friction torque to generated heat is again done by the same formula used for the friction torque due to load.

$$H_{viscous} = (1.047 x 10^{-4})n M_{viscous} \qquad (9)$$

Heat generated on the spindle bearings due to the viscosity of the lubricant are calculated for different spindle speeds and shown in   Figure 3. 7.

Total heat generated in the spindle bearings is the summation of the heat generated by the applied load and the heat generated due to the viscous friction of the lubricant. Total heat values H_{total} (W) calculated for different preloads of the spindle bearings are given in   Figure 3. 8 and   Figure 3. 9.

Estimating the heat generated by the bearings is not enough for further heat transfer calculations as the distribution of the generated heat within the bearings are also crucial

for the calculation of the heat transfer. Internal heat distribution of the bearings has always been an important decision for the researchers; several distributions are
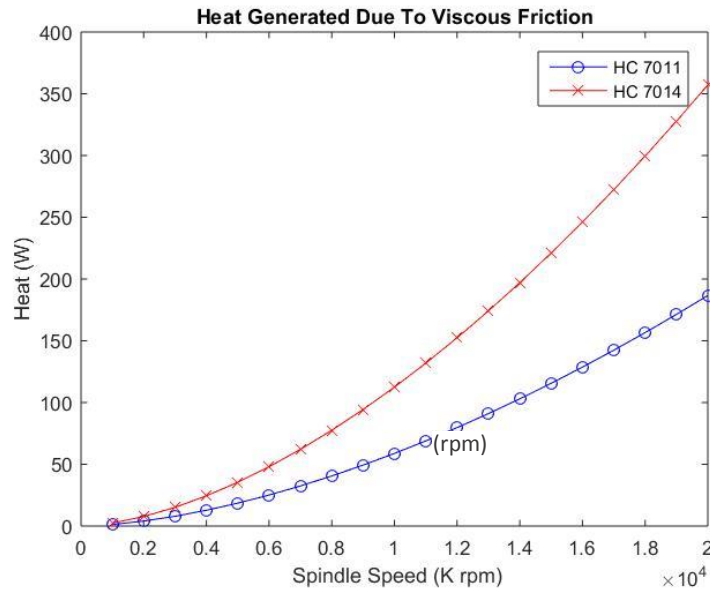
Figure 3. 7: Heat generated due to viscous friction

$$H_{total} = H_{load} + H_{viscous} \qquad (10)$$
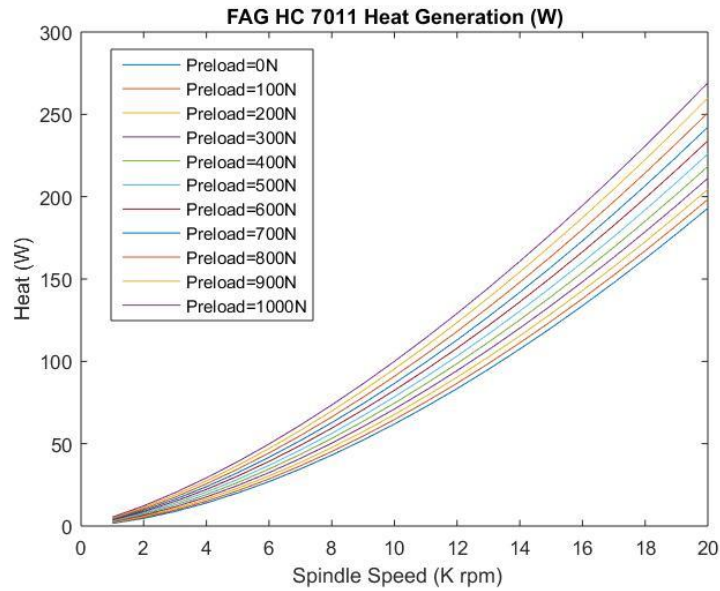
Figure 3. 8: Total generated heat for 7011

presented for the generated heat between the inner and outer rings of the bearings in the literature [32]. In this study internal heat distribution of the spindle bearings are calculated according to the masses of the inner and the outer bearing rings. Masses of

the bearing cage and balls are negligible compared to the rings, so they are excluded while calculating the heat distribution. Distribution of the total heat calculated in the
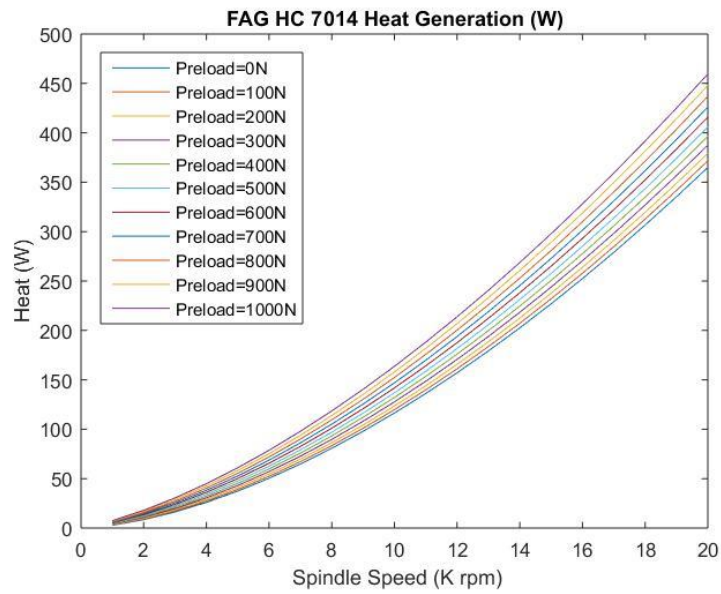
Figure 3. 9: Total generated heat for 7014

previous section is done according to the mass percentages of the rings. Percentages of the inner and outer ring masses are shown in

Figure 3. 10 calculated and distributed heats of the spindle bearings are given in Figure 3. 11.

	HC 7011	HC 7014	% Percentage:
Outer Ring Mass:	206.53 g	325.84 g	%57
Inner Ring Mass:	360.91 g	248.97 g	%43
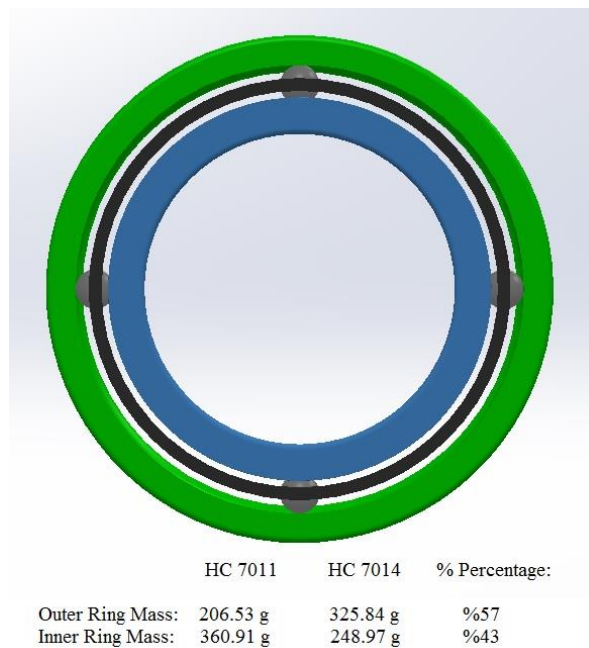
Figure 3. 10: Mass properties of the bearings
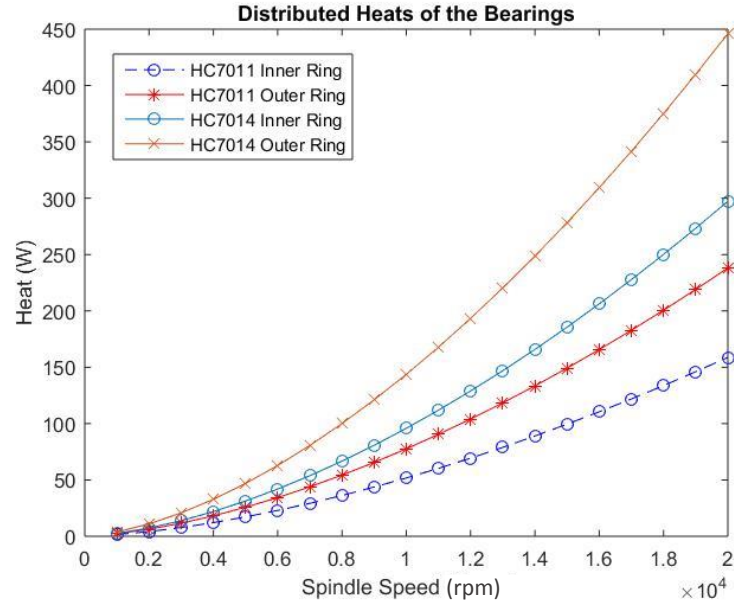
Figure 3. 11: Heat distribution of the bearings

3.4 Calculation of the Convective Heat Transfer Coefficients

One of the most important steps of thermal problems is deciding the heat transfer parameters related to the components of the system investigated. Complexity of the heat transfer problem is directly related to the system characteristics. Heat transfer can occur in three different forms; these are conduction, convection and radiation. In case of a machine tool spindle heat transfer problem, convection and conduction are the dominant transfer forms. In the first phase of the heat transfer problem, heat generated at the spindle bearings are conducted between the spindle components and this process completely depends on the material properties, i.e. heat conductivity of the spindle components. Second phase of the heat transfer problem is the convection of the heat between the spindle components and air outside the machine tool. Since the heat conduction phase will be automatically calculated according to the material properties of the components by the FE software, the only remaining parameters to be calculated are the convective heat transfer coefficients of the spindle components. Convective heat transfer of the entire spindle unit includes two different types of convections; free (natural) and forced convections. Heat transfer by free convection is used for non-moving, stationary parts of the spindle assembly; which are the parts other than the spindle shaft and bearings. Forced convection on the other hand is used in the heat transfer coefficients between ambient air and the rotating spindle. Free and forced

16

convection heat transfer coefficients are calculated similar to the approach presented by Haitao et al. [10] as shown below; but considering the flow of ambient air as totally turbulent.

Forced convection heat transfer coefficients of the rotating are calculated with the aid of three dimensionless numbers, these are Reynolds, Prandtl and Nusselt numbers of the ambient air. Reynolds number also known as the ratio of inertia and viscous forces, Re, is calculated as follows:

$$Re = \frac{u_{fluid}\, l_{shaft}}{v_{fluid}} \tag{11}$$

Parameters u_{fluid} (m/s) and v_{fluid} (m^2/s) are the velocity and the kinematic viscosity of the ambient air flowing through the spindle unit. When the convection coefficients of a cylindrical surface are calculated, perimeter of the cylinder is used as the parameter l_{shaft} (m) in the above equation. Perimeter of the spindle and the velocity of the ambient air are calculated as follow:

$$l = \pi\, d_{shaft} \tag{12}$$

$$u = \frac{l\, n}{60} \tag{13}$$

Diameter of the spindle shaft is represented by d_{shaft} (m) which is the average diameter value due to its non-uniform cylindrical shape. Velocity of the ambient air is related to the spindle speed, n (rpm), as shown in the above equation. The other dimensionless number is Prandtl number which is a material property for the air and it is calculated as 0.707 at 25 ℃ in the previous studies [22, 23]. Nusselt number on the other hand is again calculated by the following formula:

$$Nu = 0.0225\, Re^{\frac{4}{5}}\, Pr^{0.3} \tag{14}$$

The equation used for the convective heat transfer coefficient of the spindle shaft, h_{shaft} (W/ (m^{2}K)) is given below; calculated coefficients regarding to the spindle shaft in different spindle speeds is shown in   Figure 3. 12.

$$h_{shaft} = \frac{Nu\, v_{fluid}}{l} \tag{15}$$
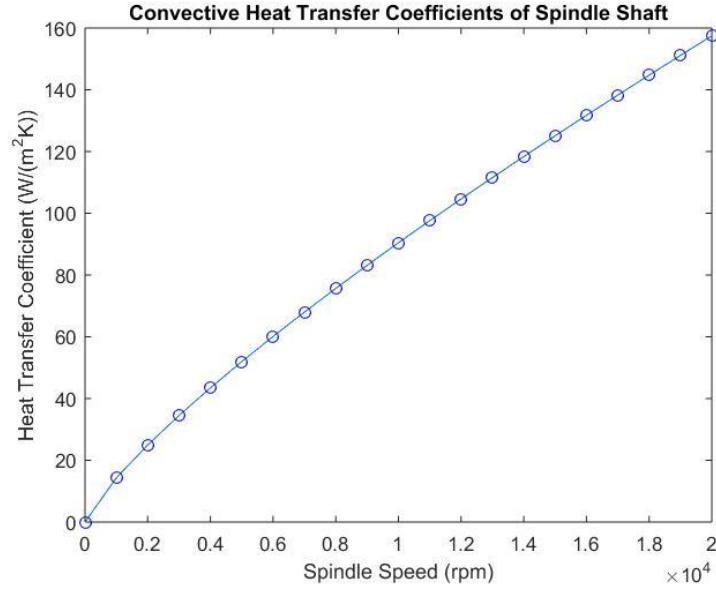
Figure 3. 12: Convective heat transfer coefficients of the spindle shaft

Free convection coefficient for the stationary (non-rotating) spindle components is taken from the literature as 9.7 (W/ (m^2K)) [10, 22, 23]. This value of the convection coefficient is calculated according to the free convection along a flat plane phenomenon [33].

3.5 Summary

In this chapter, empirical heat generation model used in this study is explained in detail. Heat generated by the bearing sets of the investigated spindle unit are calculated by using the explained model. Effect of bearing preload is shown by using different preload values for the heat calculations. Calculated heat is distributed among the inner and outer rings of the bearings with respect to their masses. Convective heat transfer coefficients are calculated for stationary and rotating parts separately. At the end of this chapter, all of the heat sources (bearing heats) and cooling parameters (convective heat transfer coefficients) are calculated for the FEM model, which is going to use these values as inputs for calculating the overall temperature distributions.

CHAPTER 4

4. FINITE ELEMENTS MODEL OF THE SPINDLE UNIT

4.1 Introduction

In this chapter Finite Elements (FE) model developed for the investigated machine tool spindle unit is presented. 3D models of the spindle components and the assembly of the entire spindle unit is explained with figures. There are several modeling blocks used to represent the different stages of the thermal deformation of the machine tool spindle; these are cooling system, temperature distribution and static deformation blocks. Details of these simulation steps and the overall modeling strategy are explained respectively. Boundary conditions of different FE model blocks, geometrical and theoretical assumptions made in order to simplify both solid model and the thermal problem, considering the solution time and accuracy constraints, are discussed. Effects of the cooling system parameters, spindle speed and running time of the machine tool spindle are investigated by comparing different simulation results. Example simulation results and screenshots are provided for better visualization of the process.

4.2 Cooling System Model (CFX-CFD)

Machine tool spindles are complex electro-mechanical systems which consume high amount of energy while generating the rotation needed for cutting tools. In the previous chapter, reasons for heat generation and temperature rise in spindle units are explained with their effect on the resultant positioning errors. Advanced cooling systems are designed to decrease the effects of generated heat and temperature rise for improving the dimensional accuracies of the machined parts. There are water, air and hybrid cooling systems, which include both water and air together as cooling fluids. The main

objective of these systems is to create heat sinks near the major heat sources of the spindle unit, such as ball bearings and spindle motor. By removing the generated heat, thermally stable environment can be achieved and the thermal elongations can be eliminated.

The cooling system of the investigated machine tool spindle in this study is a water cooling system composed of a single helical cooling channel, known as "water jacket", embedded to the spindle housing. There is an extra chiller unit outside the machine tool to cool down the water used in this cooling system and shown in Figure 4. 1. Chiller unit used in this machine tool is Rittal SK3360.475, which is a special edition, made for SPINNER, modified version of Rittal SK3360.470 series of commercial chillers [34].

Figure 4. 1: Cooling unit of the investigated machine tool

The geometry of the cooling system channels, which are embedded to spindle unit, are identified from to the 2D drawings of the spindle unit supplied by the spindle manufacturer ROYAL SPINDLES of Taiwan. FE modelling is one of the most preferred techniques for solving thermal problems with nonlinear characteristics and time dependencies. In this study in order to analyze the cooling system performance and the overall thermal performance of the machine tool spindle, FE modelling is used with the aid of ANSYS Workbench 15.0 commercial software. ANSYS is commonly used FE software for solving industrial problems and analyzing products or systems for

optimization purposes. ANSYS consist of different subsystems that are specialized for solving typical physical problems; such as thermal, structural, modal, magnetic or fluid flow problems. The complete sets of subsystems are shown in   Figure 4. 2.
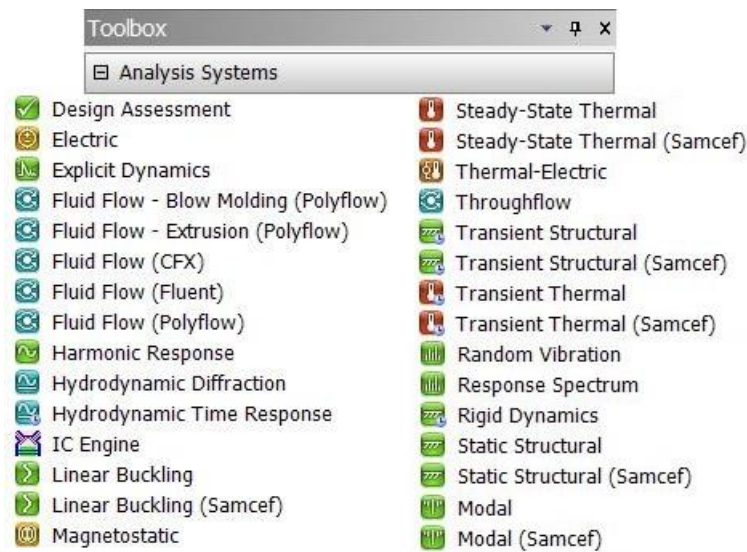
Figure 4. 2: Subsystems available in ANSYS

The reason for using this software is its ability to interchange data between different subsystems; so that even highly complex systems or problems containing more than one of the above physical problems can be simulated by using different subsystems connected to each other. In case of simulating the machine tool spindle unit, the first step of the FE model is the cooling system model; since the cooling system used in the spindle unit is a water jacket, fluid flow analysis of the cooling water passing through the cooling channels and the amount of heat absorbed by this water flow water must be computed. Modeling of the cooling system requires 3D solid models of both the machine tool spindle and cooling channels; so that the 2D section views of the spindle unit are converted to 3D solid models by using the latest version of SOLIDWORKS, 2015. Solid models of the spindle components together with the cooling system channels are given in   Figure 4. 3.

Fluid flows can be modeled by using several different blocks of the ANSYS software, which are shown in   Figure 4. 2. In this study CFX version of the fluid flow blocks is used due to its simpler user interface with respect to FLUENT for the machine tool spindle temperature modelling application. CFX module basically works on the given 3D solid model; it calculates the thermal interactions, heat transfer and fluid flow characteristics of the solid-fluid components. By using this module both steady state and

transient solutions can be calculated. In order to reduce the solution time of the CFX module of the model, solid models used in the CFX module are simplified by removing the spindle column, linear guideways and guideway carriages from the entire spindle assembly. These removed components are included in the Steady-State Thermal module.
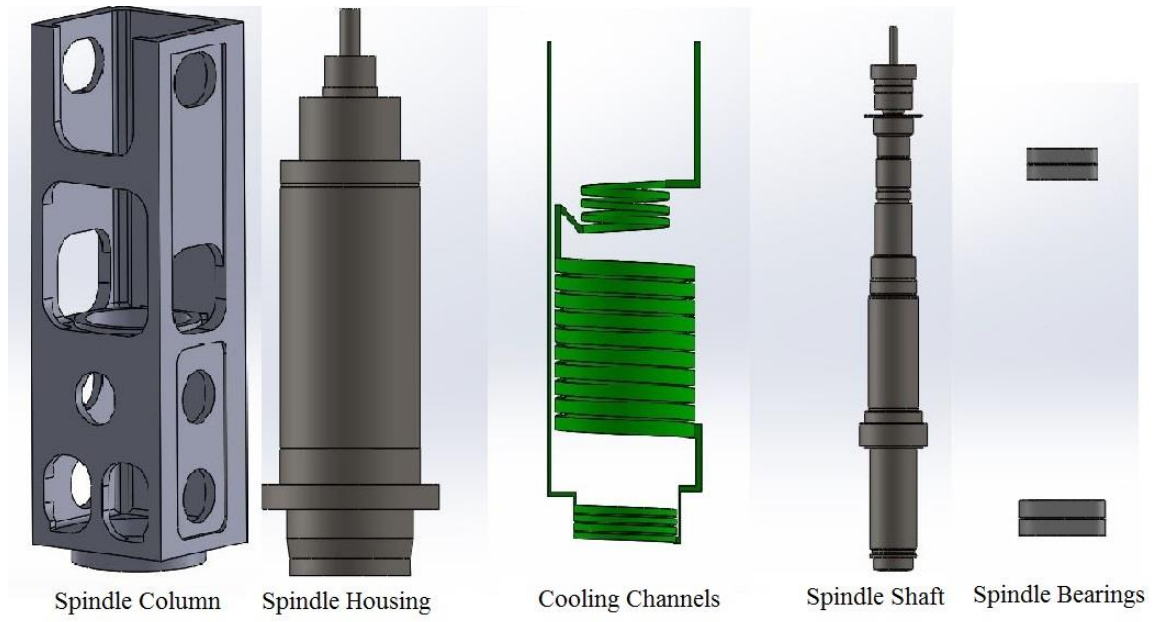
Figure 4. 3: 3D CAD model of the spindle components used in the model

Since the direct interaction of the solid and fluid domains are occur between the spindle housing, bearings, shaft and the cooling channels remaining bodies are removed from the cooling system geometry so that meshing and iterative solving steps of the largest elements, spindle column, is eliminated. Simplified 3D solid model is given as input to the first step, "Geometry", of the CFX module in the form of a STEP file. The block diagram of the used modules for the FE model of the spindle unit is shown in Figure 4. 4.

In the second step, "Mesh", of the CFX module, uploaded 3D solid model file is divided into small elements, mesh elements, so that the interactions and flows can be computed in an iterative manner between these elements. Meshing operation is done by using the auto-meshing feature of the software; this feature divides the elements according to their volumes and geometric complexity so that unnecessary meshing is eliminated. Size of the mesh elements are selected as "Medium" in order to represent relatively small components, such as bearing balls, correctly. The meshed geometry used in the

CFX model is given in Figure 4. 5. Further mesh optimization can be done to reduce the solution time of the entire model; but within the context of this thesis "mesh optimization" is not studied.
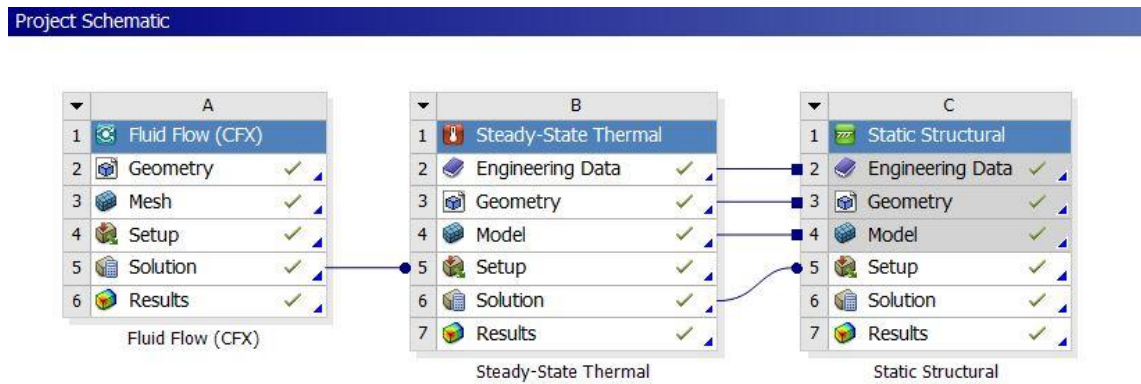
Figure 4. 4: ANSYS modules used in the model
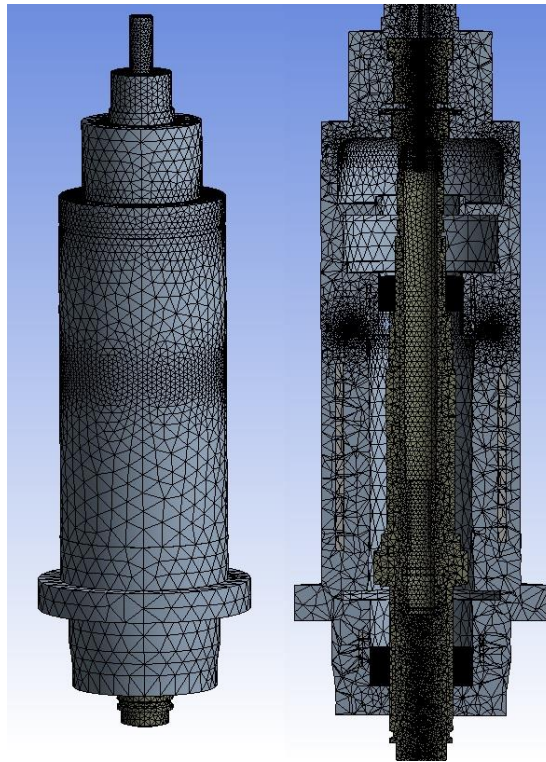
Figure 4. 5: Meshed version of the spindle housing and shaft

"Mesh" step is the place where the geometric entities are grouped for further use in the software. Grouping of the elements are done in two ways by selecting both bodies and surfaces; this grouping is very useful while selecting the fluid/solid domains, boundary conditions and inlets/outlets of the system in the "Setup" phase of the CFX module. Selection of surfaces or bodies is done according to the boundary conditions that will be

23

applied in the following sections of the model. The regions selected are basically the interfaces where heat generation and heat transfer takes place; these are mainly bearing inner/outer ring surfaces, cooling channels, shaft surfaces and spindle housing surfaces. Formed groups are shown in Figure 4. 6 exactly.

In the third step, "Setup", of the CFX module transient solution method is used with 3 minute long time steps and 30 minutes of solution duration. Transient solver time inputs
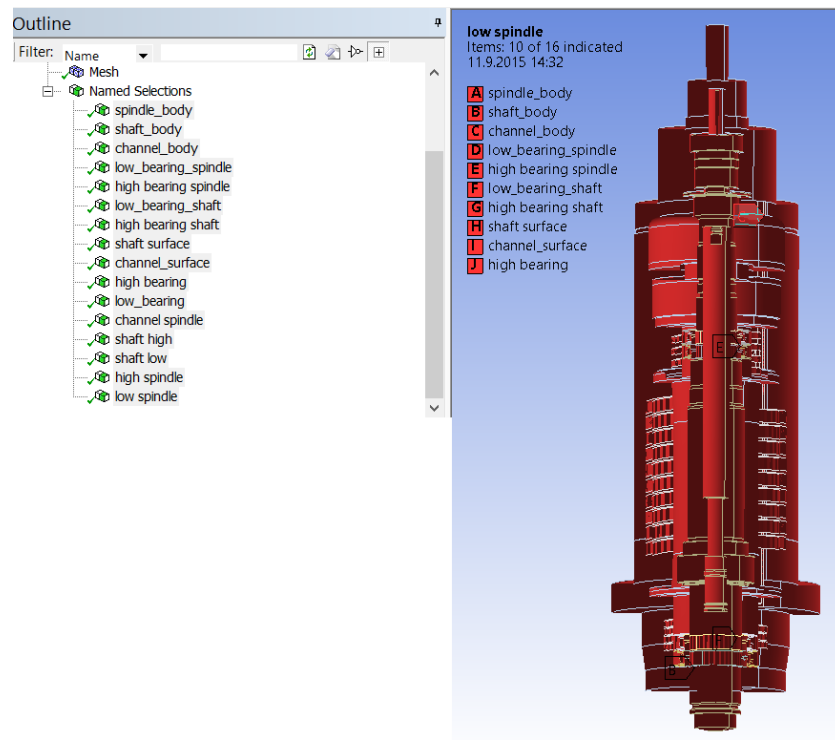
Figure 4. 6: Pre-defined regions of the spindle unit used in the model

are selected according to the verification tests, these tests are done for 30 minutes with different spindle speeds. Time step is decided as 3 minutes due to solution time efficiency after trying several other durations. Setup section is also the place where the solid and fluid domains are distinguished; previously formed cooling channel body grouping is defined as fluid domain filled with water while the remaining spindle components are defined as steel. Both domain models are defined as thermal energy in order to calculate heat transfer between them. For the fluid domain two new boundaries are added to represent inlets and outlets. According to the 2D technical drawings, inlet/outlet surfaces are chosen and shown in   Figure 4. 7. Boundary conditions

24

of the thermal problem are defined in this section. Parameters related to the cooling water flow are entered in the inlet/outlet sections. Turbulence of the cooling water is selected as "Medium" which corresponds to intensity value of %5. Speed of the cooling water is entered as 0.4 m/s according to the cooling system properties. The effect of the cooling fluid temperature entering the cooling channels is investigated by assigning different temperature values varying between 20°C to 30°C. Speed of the cooling water at the outlet is also stated as 0.4 m/s. Inlet and outlet cooling water speeds are also investigated in the optimization phase of the project by using different speed values. Domain initializations are needed for transient solution of the cooling system model; these initializations are done separately for solid and fluid domains and require initial temperatures of both domains together with the initial speed of the cooling water for fluid domain. Initial temperature of the solid domain is equal to the ambient temperature and 25°C while fluid domain is equal to the inlet temperature, which varies between 20°C to 30°C according to the simulation. Initial speed of the fluid domain is also equals to the inlet/outlet speed and 0.4 m/s.

Solid domain of the spindle unit is also separated into new boundaries same as the fluid domain; but with more boundaries. Solid domain boundaries are created for each heat generating surface and for the surfaces that are in contact with these heat generating ones as interface type boundaries. Heat generation takes place in the spindle bearings as explained in the previous chapters, so that the heat generating surfaces are the inner and outer ring surfaces of both upper and lower bearing sets. Surfaces that are in contact with the heat generating ones are the upper and lower sections of the spindle shaft, which are directly connected to the bearing inner ring surfaces; together with the upper and lower sections of the spindle housing, which are connected to the outer rings of the bearing sets. Generated bearing heat values, which are calculated and distributed among inner and outer rings of the bearing sets in the Chapter 2, are divided with the corresponding heat generation boundary area in order to get the heat flux values as W/m^2 by the written Matlab code. Heat flux values are entered under "Sources" segment of the heat generating boundaries. "Conservative Interface Flux" is selected as boundary detail for heat transfer option in the formed boundaries. Spindle shaft and remaining spindle components other than the shaft are selected as wall type boundaries
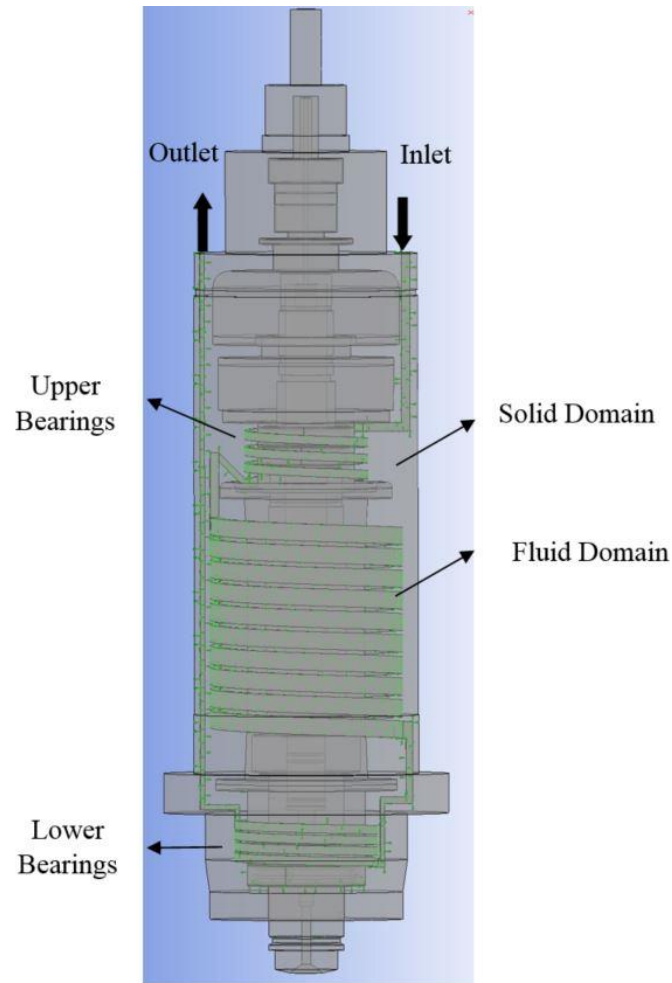
Figure 4. 7: Outline of the spindle CAD model used in CFX module

because of the convective heat transfer taking place on their surface. Convective heat transfer coefficients calculated in the Chapter 2 are used in here to represent the convective cooling. Convective heat transfer of the spindle shaft is calculated according to the spindle speed as explained in the previous chapter and entered to the "Boundary Detail" segment. Constant convective heat transfer coefficient of 9.7 (W/ (m^{2}K)) is used for the remaining spindle components again as explained in the previous chapter.

Setup step is finalized by adding the necessary interfaces to the model under the "Interfaces" tab of the model tree. Interfaces are basically the boundaries created in the solid domain as heat generating surfaces and other surfaces that are connected to them. All interfaces are created with heat transfer option enabled. In the interfaces tab boundaries which heat transfer takes place are selected, interfaces are divided into two as solid- solid and solid-fluid interfaces. Solid-fluid interface takes place between the spindle housing and the cooling channels while solid-solid interfaces are as follows:

- Upper bearing set inner ring surface – portion of the spindle shaft that is in contact with upper bearings

- Upper bearing set outer ring surface – portion of the spindle housing that is in contact with upper bearings

- Lower bearing set inner ring – portion of the spindle shaft that is in contact with lower bearings

- Lower bearing set outer ring – portion of the spindle housing that is in contact with lower bearings

- Upper and lower bearing inner rings, outer rings and bearing balls.

Model tree of the explained process, domains, boundaries and interfaces created are shown in Figure 4. 8 below.
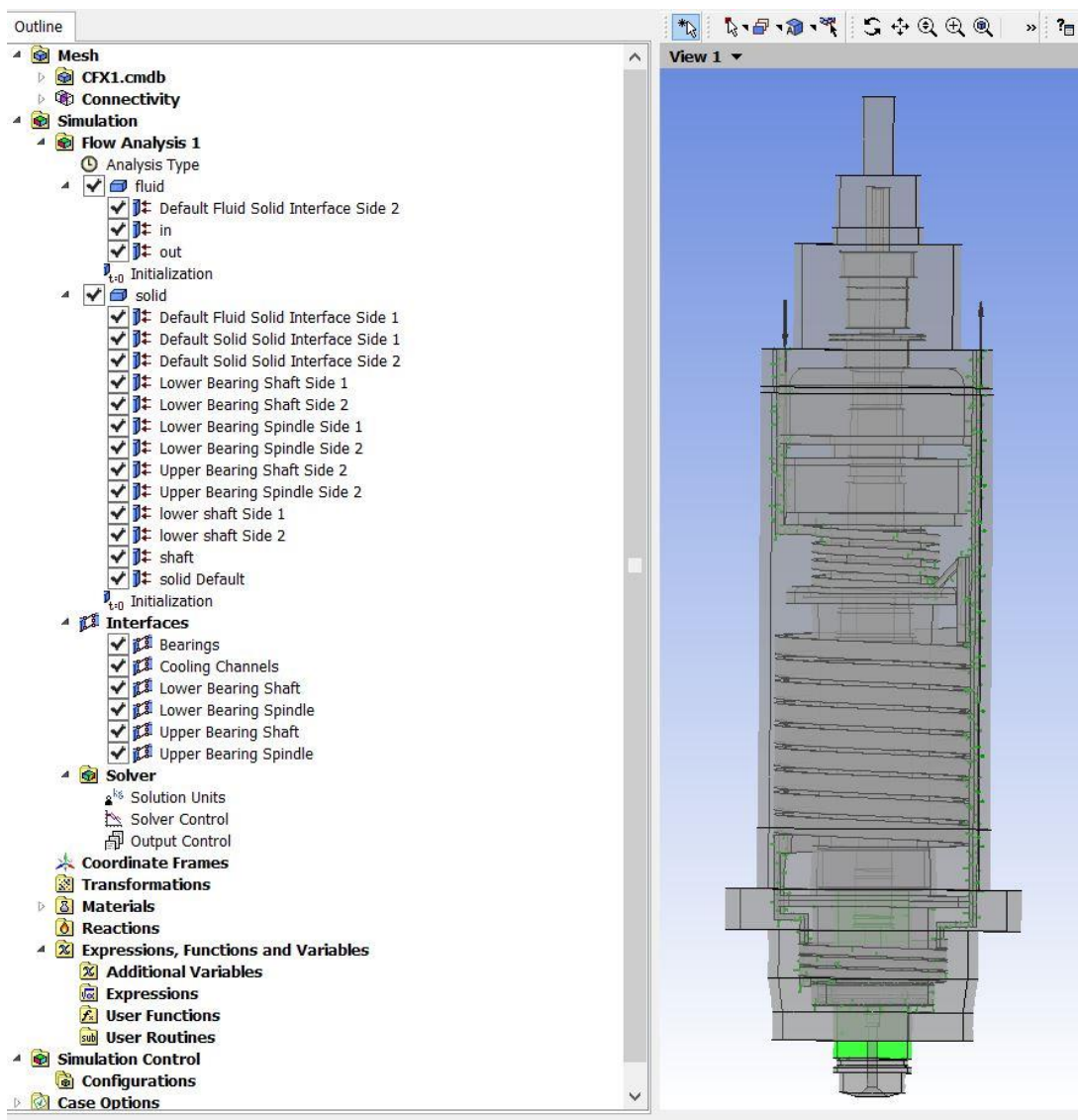
Figure 4. 8: Model tree of the CFX module

27

Last two steps of the CFX module are "Solution" and "Results", which are used for monitoring applications. Solver iterations and the calculated values of the model error together with the convergence graph can be monitored by the solution step. Results on the other hand are used for visualization of the calculated results related to the solved model. In case of the spindle unit thermal problem, final temperatures of the model components are investigated by the graphical tools provided in the results section. Physical properties such as temperature and velocity of the cooling water, spindle housing and shaft are plotted in this section.

4.3 Thermal Model

FE model developed for the Spinner U-1520 machine tool spindle unit uses "Steady-State Thermal" analysis module to calculate temperatures of the spindle components that are not included in the CFX module geometry due to the solution time optimization purposes. Thermal module is generally used for the heat transfer calculations within the given geometries. The components that are excluded from the CFX module geometry are the spindle column, linear guideways and the guideway carriages, shown in Figure 4. 9 below.

CFX Module Geometry   Spindle Column   Linear Guideways   Guideway Carriages
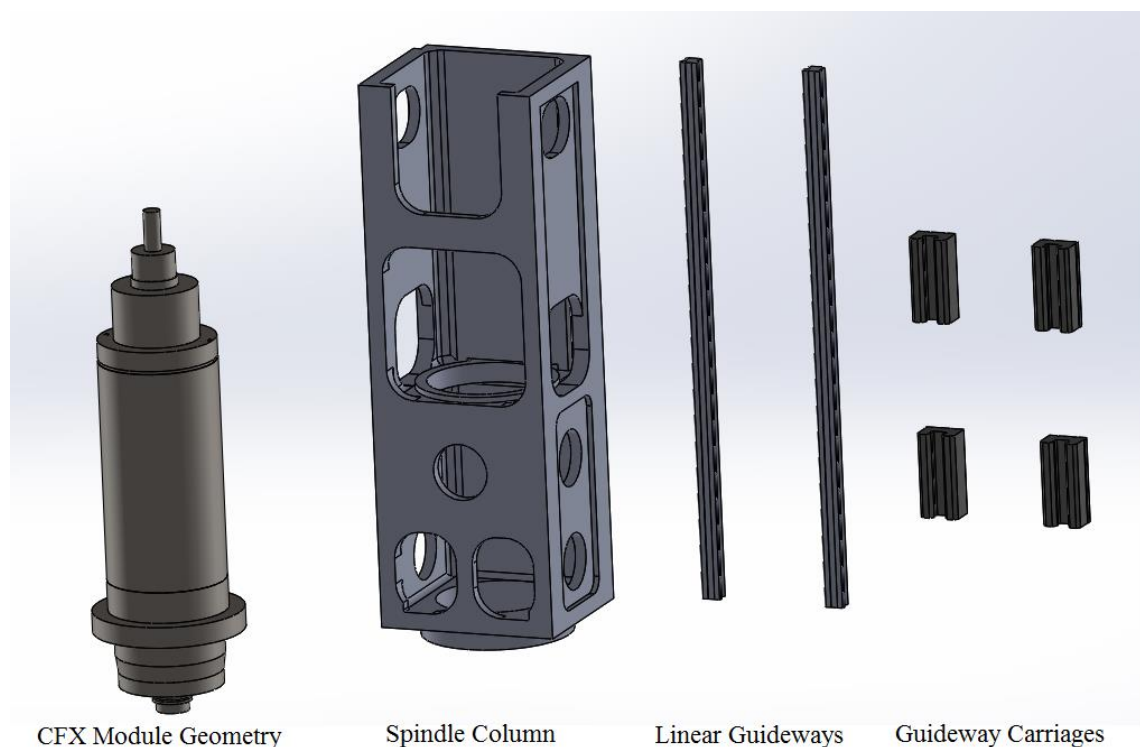
Figure 4. 9: 3D CAD models of the overall spindle unit used in the thermal module

Thermal module is connected directly to the solution step of the CFX module in order to transfer data from CFX module. The data transferred in the model is the temperatures of the spindle unit components which are calculated at the CFX module. This temperature data is used by thermal module to calculate the individual temperature distributions of the newly added components. The transferred data includes the individual temperatures of the spindle housing, cooling channels, and spindle shaft, upper and lower bearings. Temperatures transferred from the CFX module as "Imported Loads" are shown in Figure 4. 10.
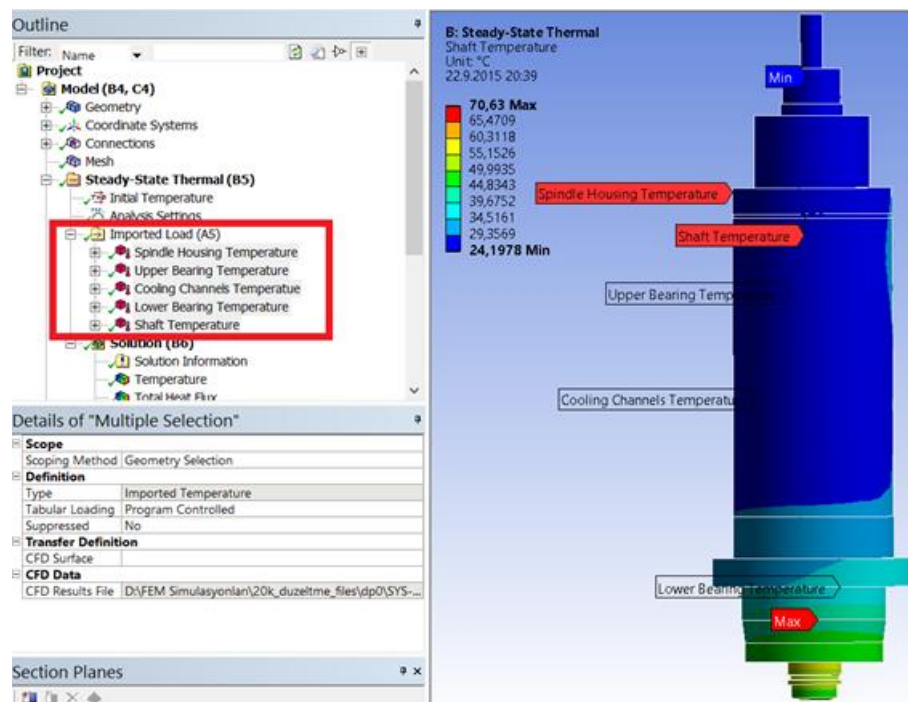
Figure 4. 10: Imported Loads

4.4 Static Structural Model

The overall aim of the developed FE model is to predict the thermal elongations of the machine tool spindle. However, the first two modules explained above are both used to find the temperature distribution of the entire spindle unit by considering the effects of the cooling system. Since the investigated elongations are due to the thermal state of the machine tool components, calculation of the heat distribution is crucial. The next step after calculating the temperature distribution is to determine the elongations caused by the temperature distribution. Static Structural module used at the end of the project scheme as the third module calculates the thermal elongations of the spindle unit components. Physical boundary conditions, such as gravitational force acting on the

system, support structures that hold the spindle unit or stiffness constraints used in spindle components are all introduced to the FE model in this module. There are three new boundary conditions added to the system, these are:

- Gravitational force acting on all spindle unit in the Z direction,
- Fixed supports over the four linear guideway carriages, which are the only connections between the spindle unit and rest of the machine tool,
- Elastic supports for the upper and lower bearing sets, in order to limit the movement of bearing sets according to the physical assembly structure.

Upper and lower bearing sets have different stiffness values both because of their sizes and installation techniques. Lower bearings are mounted between the spindle shaft and spindle housing using tight fitting, which disables the axial movement of the bearing sets completely. Upper bearing sets on the other hand are fitted to the system tightly but allowed to move in the axial direction within 200 μm range. This movement is allowed by the constant preloading mechanism used in the spindle assembly. 10^3 N/mm^3 and 10^4 N/mm^3 stiffness values are applied to upper and lower bearings respectively as elastic supports. Results of the Static Structural module are the thermal deformations calculated for all elements in the spindle unit. Sample results are shown in Figure 4. 11.

Figure 4. 11: Example results of the Static Structural Module

4.5 Model Simulations

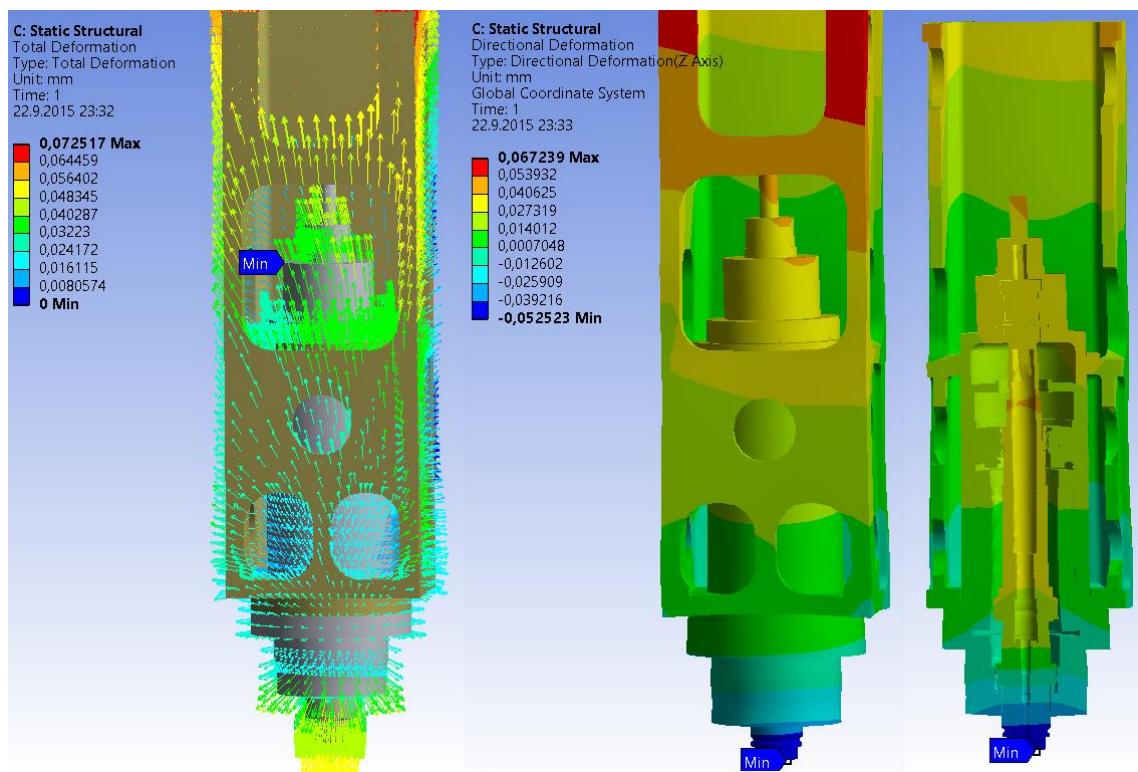The FEM model is used to simulate several tests for comparison of the results to check the prediction accuracy. The tests that are simulated with the model are the short duration tests of 30 minutes and 5000-10000-15000-20000 rpms of spindle speeds. Detailed results of the FEM model simulations using these 4 different test parameters are given below.

a) Cooling Water Temperatures

CFX module of the FEM model calculates the final temperature of the cooling water, which flows inside the cooling channels of the spindle assembly. After all heat transfers are done, temperature distributions of the cooling water for the different spindle speeds are shown in Figure 4. 12. Temperature of the cooling water increases as it flows through the channels towards the bearing sets. According to the design of the cooling system, cooling fluid enters the spindle unit form the top side, it travels all the way down to the very bottom of the spindle unit and finally travels all the way back and exit from the top side again. By following this sequence, the components that are cooled are upper bearing set, spindle housing and the lower bearing set respectively. The problem with this sequence is that the lower bearings, which are the last components in the cooling sequence, are the most powerful heat sources of the entire system due their larger diameter than the upper bearings. Trying to cool down the most powerful heat sources by already warmed up cooling fluid is resulting in higher temperatures in the lower side of the cooling channels. Upper bearings on the other hand are smaller in diameter compared to the lower ones and generating less heat; however due to the current design of the cooling system they are the best cooled components. It is going to be perfect if this sequence is directly inverted. Another importance of this mistake in the cooling sequence is that the lower bearings are the closest heat sources to the cutting tool; so that the lack of cooling observed on these bearings will directly be seen as higher temperatures and higher thermal deflections on the tool.

a) Spindle Shaft Temperatures

Spindle shaft is one of the most important components of the spindle assembly due to its rotation and direct connection to the tool tip. Spindle shaft is the only component within

the spindle assembly which does not have built-in cooling channels. Cooling of the spindle shaft is achieved by the bearings which are the only structures that connect spindle shaft to the rest of the spindle assembly. The lack of cooling system is combined with the direct connection to the main heat sources of the system, bearings, and making the spindle shaft the hottest component of the entire assembly. Locations around the bearing inner rings are expected to be the hottest regions on the shaft. Spindle shaft temperatures calculated for different spindle speeds are given in Figure 4. 13 below. As in the cooling water simulations, shaft temperature increases with the increasing spindle speed and bearing locations on the shaft are the hottest regions as expected.

a) Spindle Surface Temperatures

Temperatures of the entire spindle surface are also calculated by the CFX module within the FEM model. Spindle outer surface is cooler compared to other parts of the assembly because of its distance to the main heat sources and the convectional heat transfer taking place between the outer surface of the spindle and the air outside. Calculated temperatures of the spindle surface are given in Figure 4. 13. These figures show the spindle inner surface which is in contact with bearing outer rings. High temperature values seen at the legend belong to the bearing rings. The effect of the spindle speed is again obvious on the temperatures which increase with the spindle speed.

Temperature prediction results for four different tests are compared on a single graph given in Figure 4. 15, showing the effect of spindle speed. Cooling water temperatures are lower than the shaft and spindle temperatures according to the graph. The reason for shaft and spindle surface temperatures being so close to each other is their direct connection to the spindle bearings, which are the only heat sources of the spindle system. Outer bearing rings are connected to the spindle housing while the inner rings are attached to the shaft. As explained in the previous chapter, outer rings of the bearing sets receive %60 of the total generated heat and the small temperature difference between the shaft and spindle surface is due to this partitioning of the heat between the bearing rings.
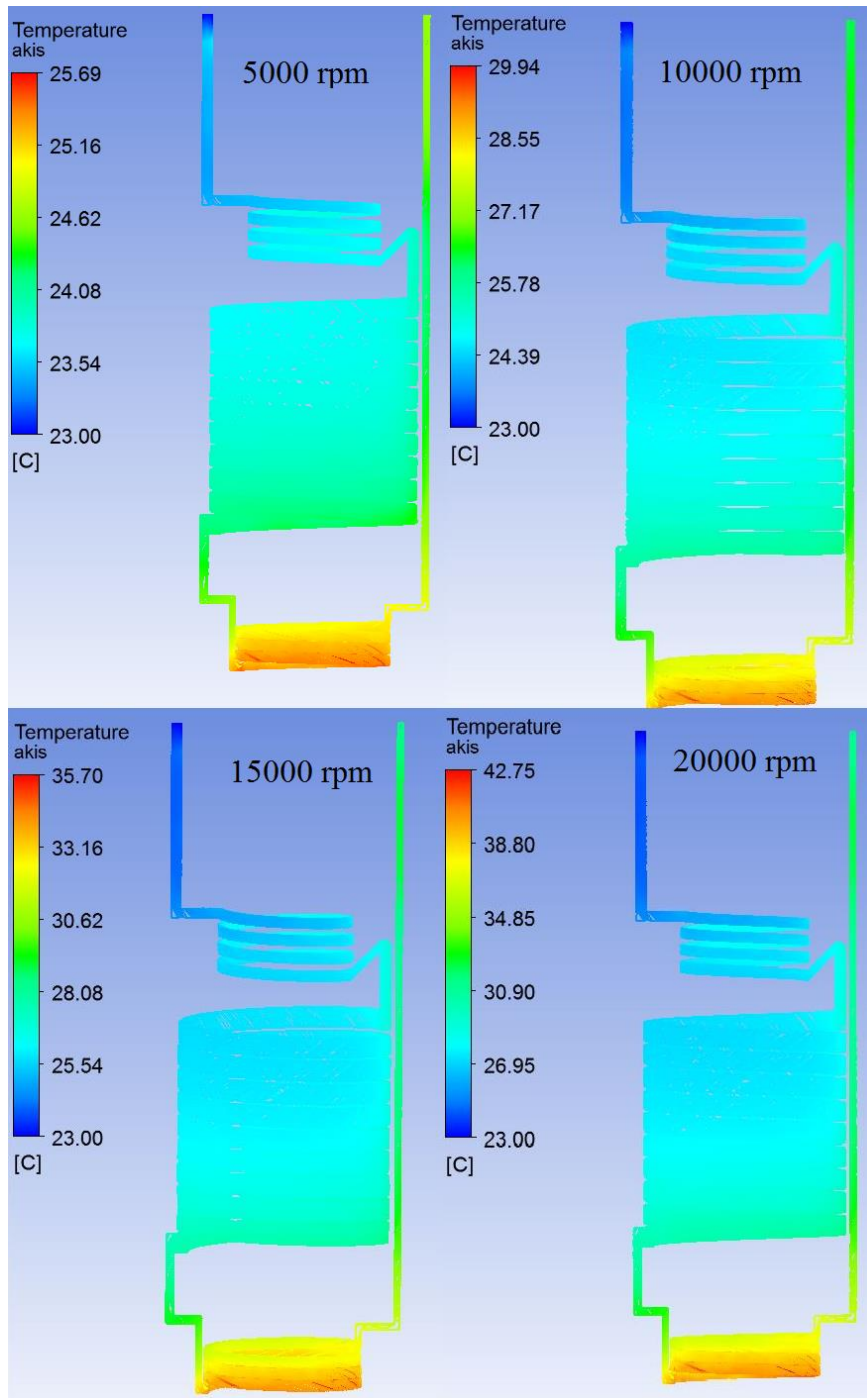
Figure 4. 12: Temperature of the cooling fluids within the cooling channels for different spindle speeds
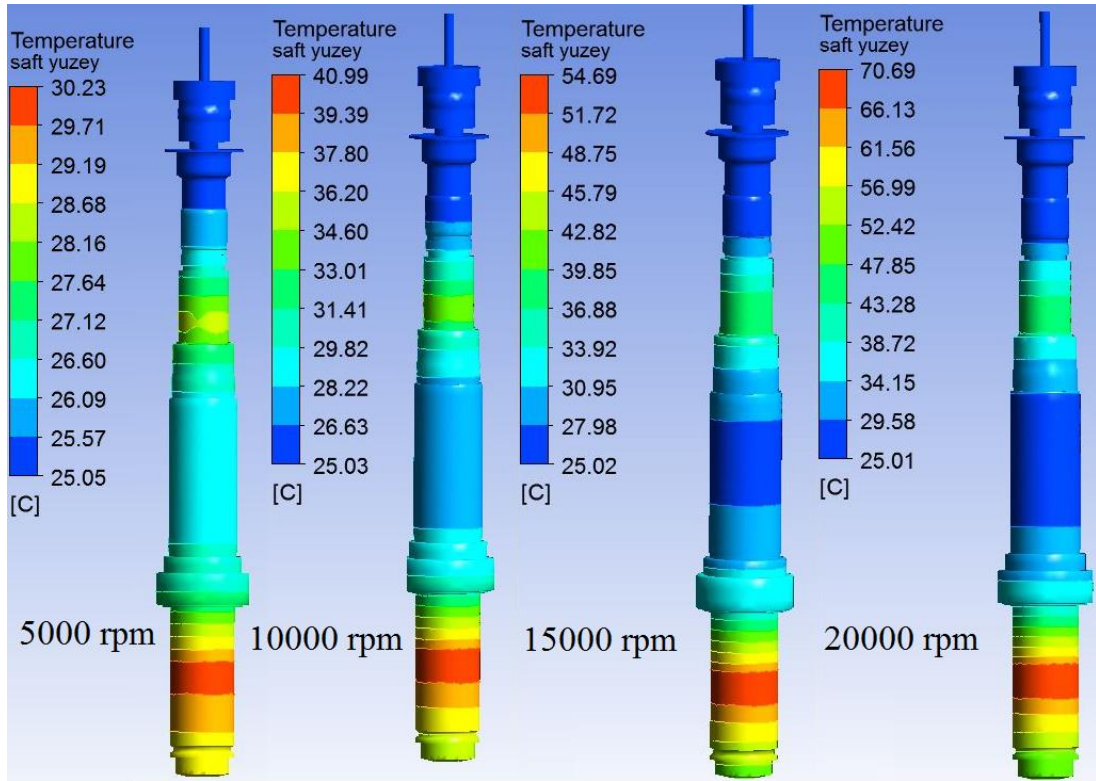
Figure 4. 13: Calculated temperature distributions of the spindle shaft for different spindle speeds
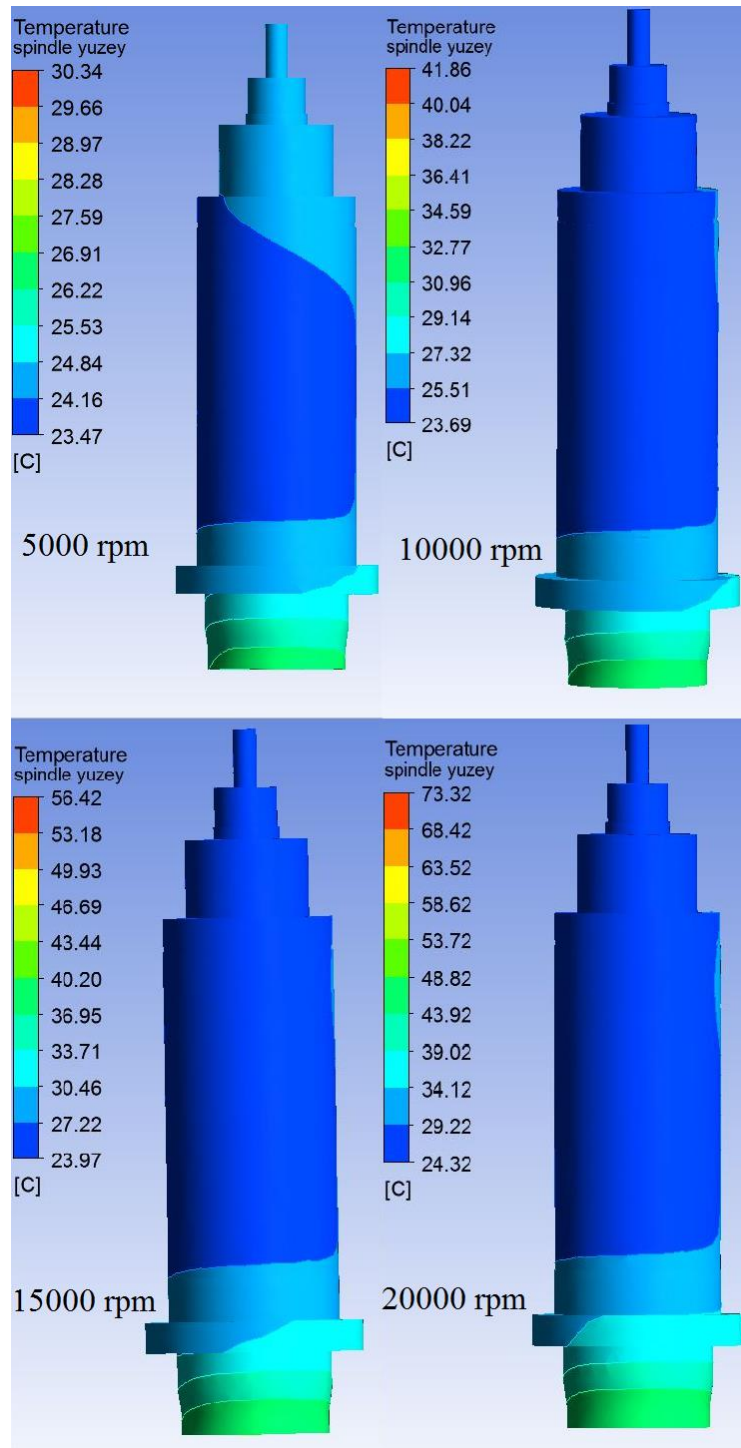
Figure 4. 14: Calculated temperature distributions of the spindle surfaces for different spindle speeds
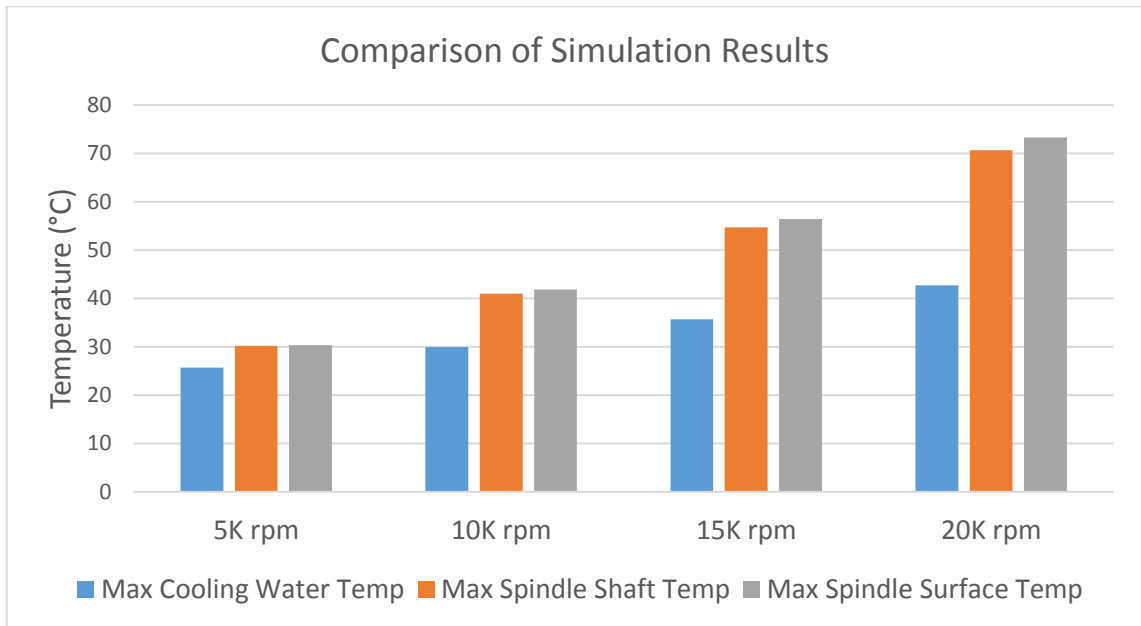
Figure 4. 15: Comparison of the different spindle speed simulations

b) Deflections of the Tool Tip

Predicting the thermally induced elongations of the tool tip is the main objective of the FEM model used. According to the calculated temperature distributions, deflections of the tool tip are calculated by the model for different spindle speeds and the results are given in Figure 4. 16 below. The deflection of the tool tip along the Z axis increases with the spindle speed. With the increasing spindle speed heat generated by the spindle bearings is increases and causing higher temperature distributions over the entire spindle components. As a result of these higher temperature distributions, tool tip deflections are also increasing accordingly. The nonlinear relationship between the spindle speed and tool tip elongations is given as a chart for visualization of the results in Figure 4. 17.

4.6 Summary

In this chapter, FEM model developed for the calculating the temperature distributions and thermal deformations are explained in detail. Modules used in the FEM model are explained one by one including the inputs and outputs of each. 3D CAD models used in each module are presented. Connections between the all three modules used in the FEM
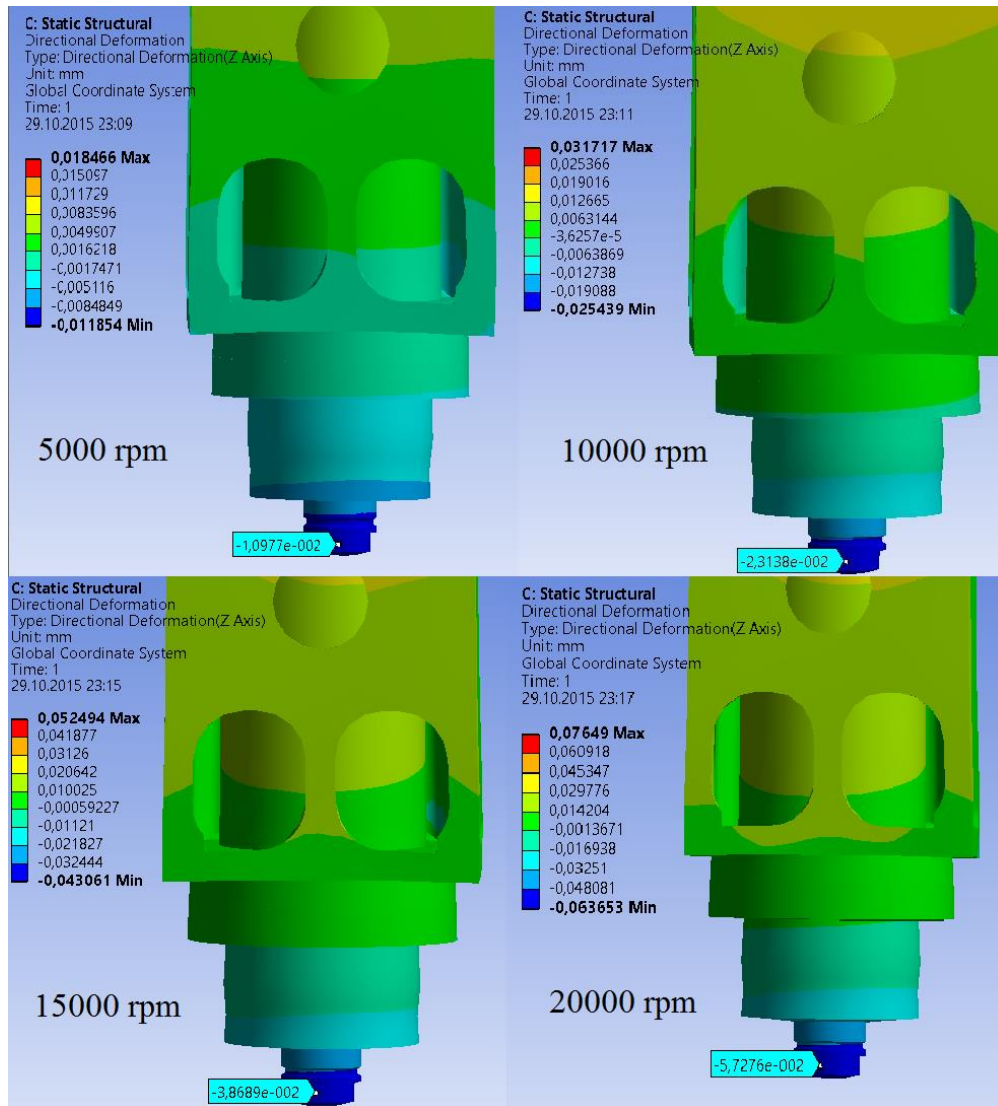
Figure 4. 16: Z-direction deflections of the tool tip for different spindle speeds
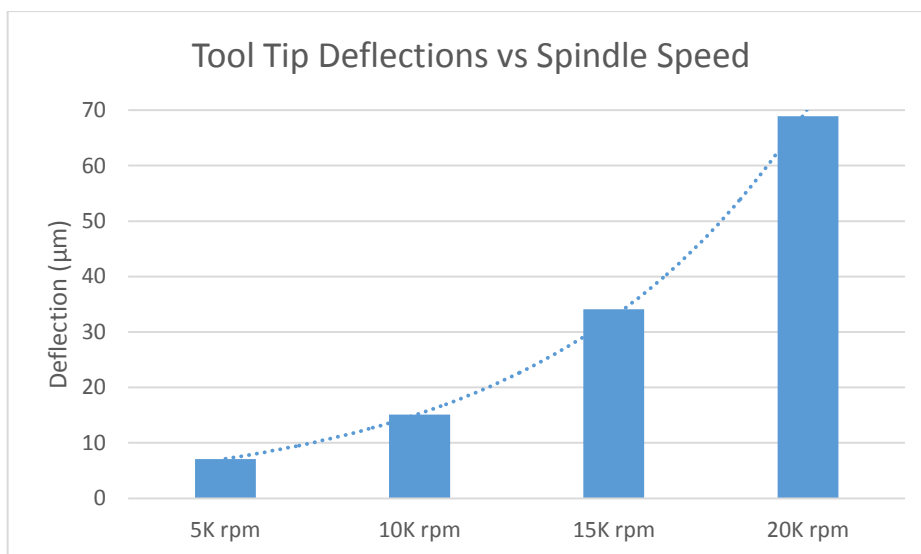
Figure 4. 17: Comparisons of the tool tip deflections for different spindle speeds

model are again explained by presenting the transferred information. In the last part of the chapter, simulation results obtained by the proposed FEM model are shown for four different spindle speeds. Two important outputs of the model are the temperature distributions and the tool tip deflections due to the thermal affects. Simulation results will be used for model validation in the upcoming chapters.

CHAPTER 5

5. EXPERIMENTAL RESULTS AND VERIFICATION OF THE SPINDLE
THERMAL MODEL

5.1 Introduction

In this chapter experimental set-up and measurement devices used throughout the study
are presented with the measurement procedures. In order to validate the prediction
performance of the developed FE model, several spindle warming tests are carried out
for measuring both spindle temperature and tool center point displacements. Warming
tests are carried out by considering both ISO recommendations and
mechanical/electrical limitations of the machine tool investigated. Results of these tests
are compared with the simulation results taken from FE software and the prediction
accuracy of final temperatures and thermal elongations related to the spindle unit
components are calculated. Details of the measurement equipment, data acquisition
system used, pre and post data processing steps are explained. FE model simulation
results, spindle unit temperature measurements and tool center point displacement
results for all of the tests done are presented together with the explanations and graphs.
Screenshots and pictures of the experimental set-up and used software are provided.

5.2 Experimental Set-up

Thermal performance evaluation of a machine tool spindle unit consists of several
different measurements related to the investigated spindle unit; such as temperature
measurements of individual spindle elements, cooling fluid temperatures, environmental
temperature together with the thermal elongations measured in 3 dimensions at the tool

tip. Conventional temperature measurement techniques are generally based on placing thermocouples to the locations where the temperature data is needed; so in the case of a machine tool spindle unit that consists of so many parts these conventional techniques become really complicated and time consuming. Since spindle units are completely sealed systems, embedding temperature sensors within the bearings or shaft is both complex and risky for liquid leakage; due to this reason temperature measurements are taken from the external component surfaces. The usage of infrared camera for the external temperature measurements of the spindle unit components is one of the novelties for this study. Infrared cameras are mostly used for the temperature monitoring of different cutting processes such as turning, milling or grinding in the machine tool literature; but they can also be used for the entire machine tool thermal performance tests. The advantages of using infrared technology are:

- Quick and easy installation: reduced set-up time.
- Contactless measurement capability: safer for high speed applications.
- High accuracy: provides robust measurement results.
- Large measurement range: perfect for entire machine tool measurements.
- Easy post-processing of the data: reducing the analysis time.
- Easy real time monitoring/ visualization: perfect for locating the most/least heating regions via images.

Infrared camera used in this research is FLIR A325 together with the measurement software FLIR ThermaCAM Researcher Pro as shown in Figure 5. 1. Before using the infrared camera in the thermal measurements, emissivity settings of the measurement software is calibrated for the spindle unit components by using four J-type thermocouples to measure temperatures of the spindle unit components and then correct the emissivity value of the infrared camera. All of the temperature measurements in this research are done by using the calibrated infrared camera including spindle component temperatures and environmental temperatures.

Temperature plots given in this section are all showing the temperatures of dominant (most heating) measurement points. An example temperature measurement file from the ThermaCAM Researcher Pro software is provided in Figure 5. 2.

The first part of the thermal performance tests was the temperature measurements that are done using infrared camera; second part of the thermal performance measurements

is the precise and accurate measurement of the thermal elongations at the tool tip. Since the investigated machine tool is a 5 axis machine tool and the orientation of the tool tip

Figure 5. 1: FLIR A325 Infrared camera used in the measurements
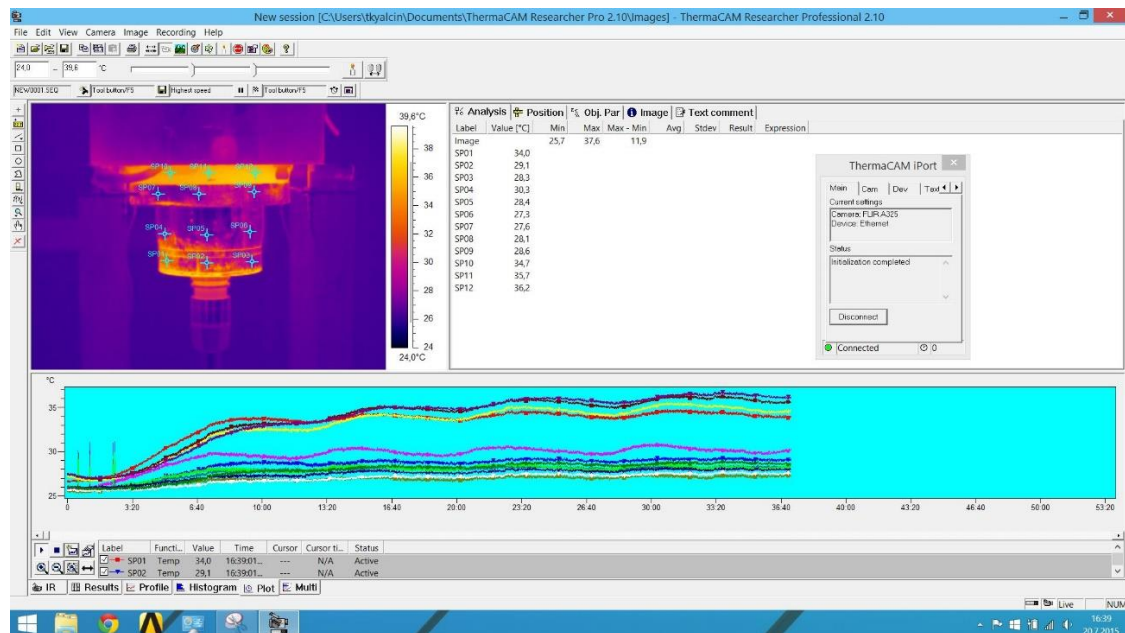
Figure 5. 2: Example of a temperature measurement file

is very important for the part dimensions, elongations at the tool tip are measured in 3 dimensions. For the thermal elongation measurements non-contact Eddy Current displacement sensors are chosen according to the similar applications done in literature and recommendations of ISO 10791-10 [35]. Displacement sensors used in the study are Micro-Epsilon NCDT 3001 series sensors as shown in Figure 5. 3 below. Three dimensional measurement of the tool tip requires at least 5 displacement sensors in order to measure the lead and tilt movements of the tool tip accurately. These 5

individual sensors are positioned by several special measurement fixtures designed for different tests and they are connected to the PC via data acquisition system. The displacement sensors and the measurement fixtures used throughout the study are shown in Figure 5. 4. Sensors are powered by a 24V power supply externally.

Figure 5. 3: NCDT series displacement sensors

Temperature data is acquired by the infrared camera software; however for the displacement sensors additional data acquisition system is needed in order to convert analog voltage data to corresponding distance values measured in real time. For this purpose National Instruments DAQ software LabVIEW is used with NI 6259 BNC board that displacement sensors connected directly to it. BNC board is than connected to the measurement PC via USB and the displacement values of each sensor is monitored and saved in real time by the developed LabVIEW template and GUI. Distance measurements from all five sensors are plotted on separate graphs with respect to time. Noises in the displacement measurements are post-filtered again by using the LabVIEW and MATLAB with several curve fitting and statistical averaging methods.

Thermal performance of the machine tool is measured by conducting several spindle warm-up tests that are taken from both previous researches listed in the literature and recommendations stated in the related parts of ISO test for machine tools. The differences of these tests are basically the spindle speed used during the test and the test duration; because spindle speed and running time of the spindle unit are known as the most important factors causing the heat generation and temperature rise in machine tools. Tests done in this study can be categorized as constant and variable speed tests. Constant tests are divided into two according to the test duration as 90 and 30 minutes long tests while the variable speed tests are done according to the procedure stated in

ISO standards. As shown in the Figure 5. 4 measurement set-up, two different tools used during the deflection tests. These tools are standard HSK-63 test mandrel and
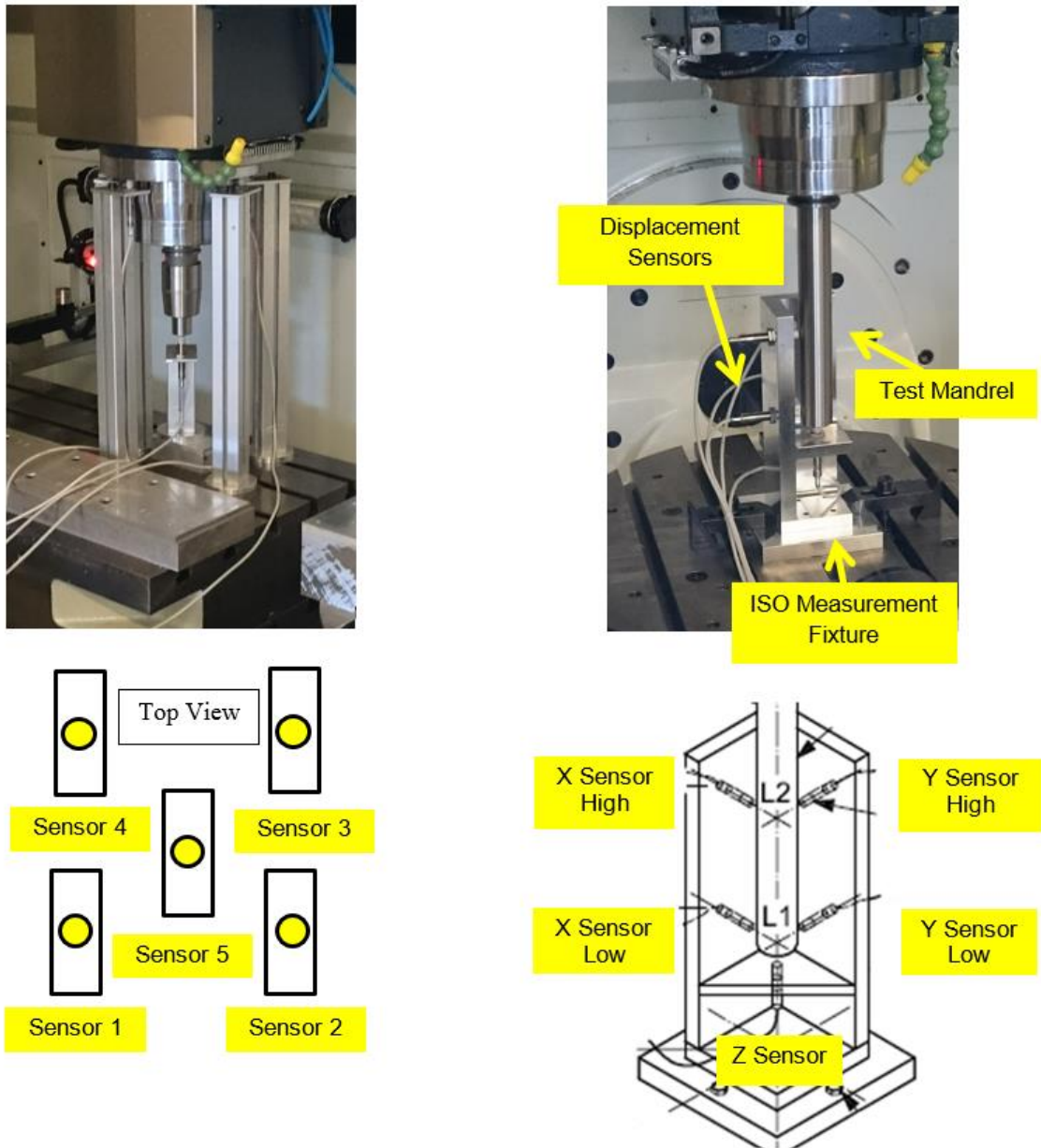
Figure 5. 4: Displacement measurement set-up and fixtures

40 mm long steel block with 32 mm diameter clamped to a tool holder. Test mandrel is used in the early tests for determining the deflection of the tool in 3 dimensions; but after these early tests it is concluded that the thermal elongation of the tool is mostly in the Z direction. Since rotating the test mandrel, which is 300 mm long, with 20K rpm is not safe enough for both machine tool and the majority of the deflections are measured

in the Z direction; after first couple of tests, test mandrel is replaced with the steel block.

5.3 Constant Spindle Speed Tests Results

Constant spindle speed tests are done using the experimental set-up explained in the previous section. Two different time durations are used in these tests, 30 and 90 minutes. One of the reasons for conducting tests with different durations is to observe the effect of spindle running time on the spindle temperature distribution and thermal elongations of the spindle components. Another reason for choosing different durations for the tests is to be able to compare the results of these tests with the FEM model simulation results; since transient solvers are used in the FEM model, simulating longer durations, like 90 minutes, is very time consuming because of the computational complexity of the thermal problem. Longer duration tests on the other hand are needed for the evaluation of the overall temperature performance of machine tools considering the fact that machine tools can be used 10 to 24 hours a day continuously. For the longer duration tests, in order to see the cooling characteristics of the spindle unit temperature and deflection measurements are continued after stopping the spindle unit. 90 minutes of warming cycle is followed by 90 minutes of cooling phase and the results of these two phases are compared.

    5.3.1 Longer Duration Tests

The initial step of thermal performance evaluation of the spindle unit is a 3 hour long spindle warming and cooling test. During the first 90 minutes of this test spindle runs at the maximum speed of 20,000 rpm while test mandrel is attached to it. After 90 minutes spindle is stopped and waited for another 90 minutes to cool down. All five Eddy Current displacement sensors attached to the ISO measurement fixture were measuring the distance between the fixture and rotating test mandrel throughout the warming and cooling phases. Displacement graphs of all sensors and the temperature graph of the spindle unit during the test is given below.

    a) Heating Phase Results

Infrared camera images taken every ten minutes are given in Figure 5. 5 for visualization of the temperature distribution within the spindle components.

44

Identification of the hottest parts within the spindle assembly is again done using these figures. Since it is easy to add many measurement points from the infrared camera software, temperature measurements are taken from 10 different locations and plotted. Temperature plot is given in Figure 5. 6 below. According to the temperature plot maximum temperature recorded during the heating phase is 36,7°C with a starting temperature of 26,9°C, which is plotted in green. Location of the hottest point is shown with a green circle on the t=0 image of Figure 5. 5. Maximum temperature difference of 9,8°C is measured for 90 minutes rotation of spindle at the maximum speed of 20K rpm.
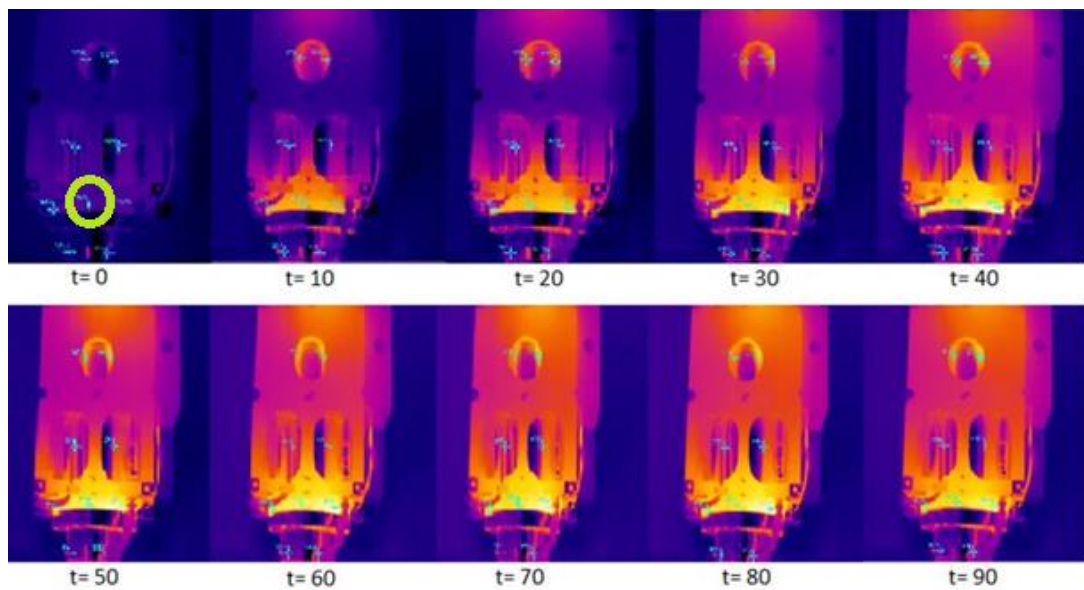
Figure 5. 5: IR camera images of the measured temperatures
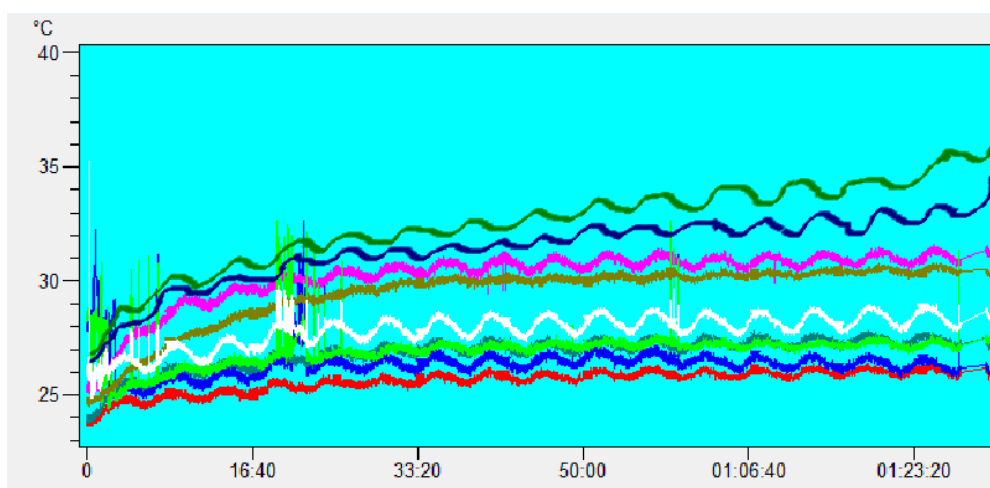
Figure 5. 6: Temperature plot of the heating phase

Deflection measurements recorded during the heating phase with five sensors, post processed (noise free) displacement results are given in Figure 5. 7 together with the calculation of the maximum deflections measured by each sensor. It is obvious that the deflection in the Z direction is huge compared to other directions. X axis deflection is considered as negligible, however deflection in the Y axis is also large enough to consider as a problem. The reason for the larger deflections in the Y direction compared to X is the configuration of the machine tool, since the Z column is mounted on to the Y column; whole spindle unit is supported only from the Y direction. Thermal elongation of the spindle unit causes a bending effect around the support and test mandrel deflects more in the Y direction as shown in Figure 5. 8.

Figure 5. 7: Post-processed deflection measurement results of the heating phase

Figure 5. 8: Schematic of the bending motion along Y direction

b) Cooling Phase Results

Machine tool spindle is stopped after the first 90 minutes and measurements are continued for another 90 minutes to see what happens in the cooling phase. It is expected for the test mandrel to fully recover its deflections in all directions during the cooling phase. Temperature measurements of the cooling phase are given in Figure 5. 9 below. Temper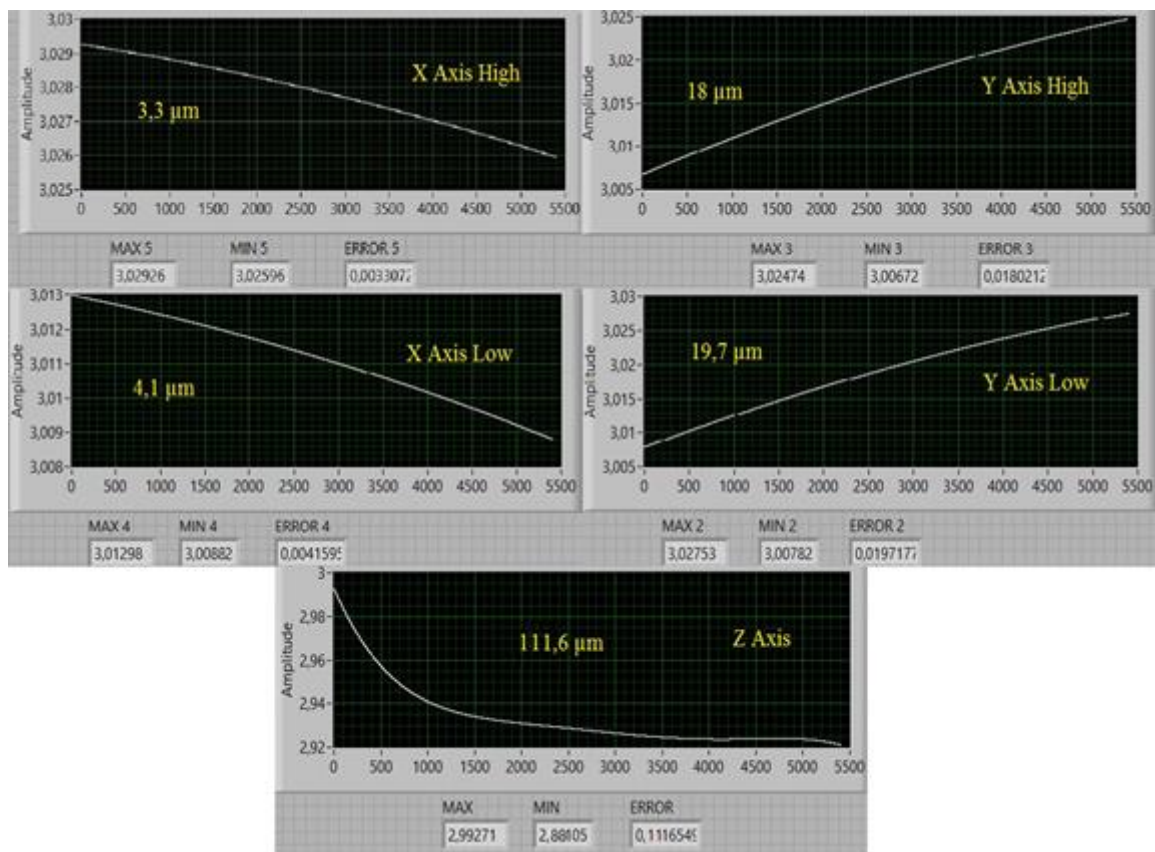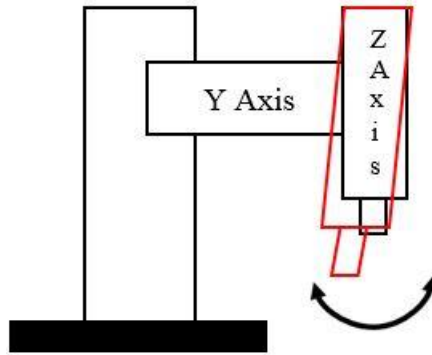atures of all points rapidly started to decrease after stopping the spindle rotation and initial temperatures were maintained during the cooling phase. Temperature plots of both heating and cooling phases of the spindle unit have periodic fluctuations which are due to the cooling system. Cooling system used in the machine tool runs on a set point control scheme; which basically starts to cool cooling fluid if its temperature rises 2°C from the set temperature and stops cooling when the temperature of the cooling fluid drops 2°C below the set temperature. This set point control mechanism explains the periodicity of the measurement point temperatures plotted for the entire 3 hour test. It is observed that the cooling system fluctuations have larger periods of 15 minutes in the cooling phase, while they were 6 minutes in the heating phase of the test.

Deflection results of the cooling phase are recorded to see if there are any differences between heating and cooling characteristics of the spindle unit. According to the post-processed deflection graphs shown in Figure 5. 10 below, deflections in X and Z directions are fully recovered in the cooling phase; however there is a significant difference in the Y direction measurements of both phases. %40 of the Y direction deflections are recovered according to the test results.
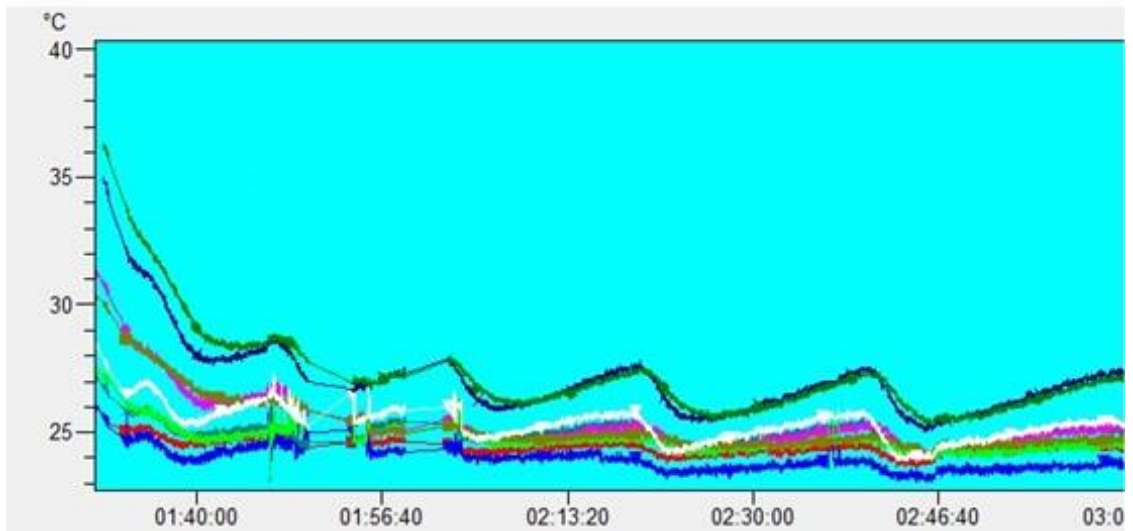
Figure 5. 9: Temperature plot of the cooling phase
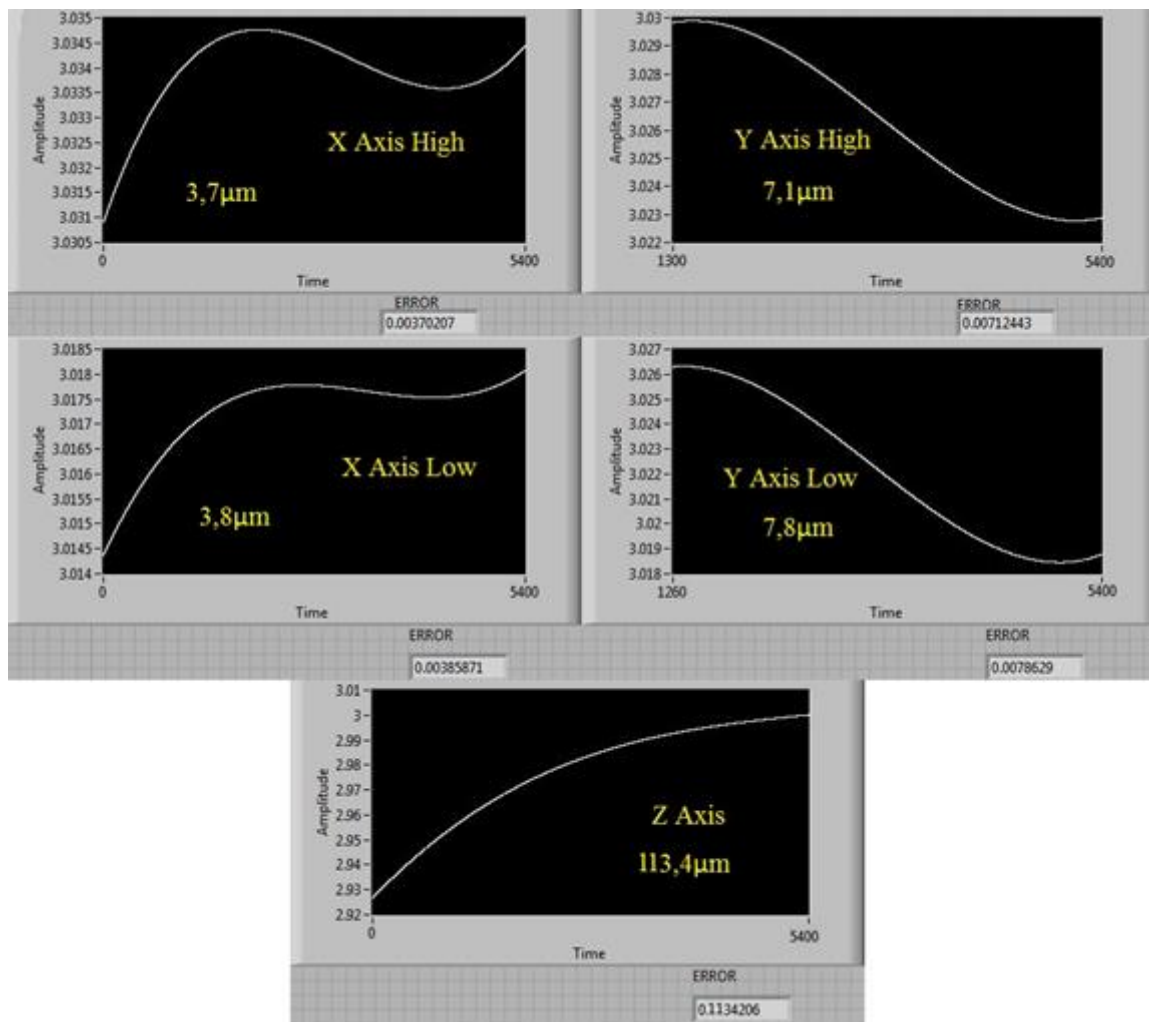
Figure 5. 10: Post-processed deflection measurement results of the cooling phase

48

5.3.2 Shorter Duration Tests

Longer duration tests are conducted to see the thermal behavior of the spindle unit with respect to time; however in order to validate the FEM method explained in the previous sections tests with shorter durations are needed. Transient solver used in the FEM model is time dependent and simulating longer durations, such as 90 minutes requires exponentially increasing solution times. 30 minutes of spindle warming tests with 5K-10K- 15K and 20K rpm spindle speeds are used as shorter duration tests in this study. Temperature plots of the shorter duration test are given in Figure 5. 11. Statistics of these four tests are plotted in Figure 5. 12 to show the effect of spindle speed on measured temperatures. Maximum measured temperatures increase with the spindle speed.
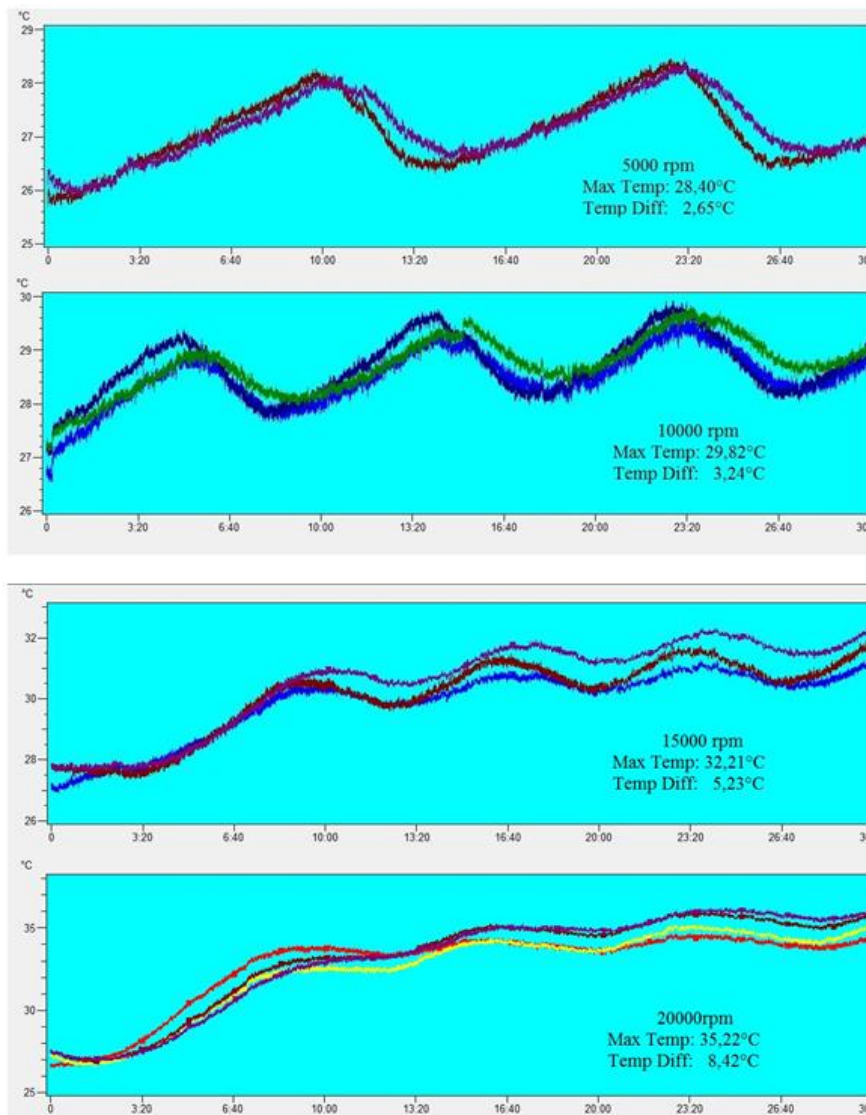
Figure 5. 11: Temperature measurements of the shorter duration tests

The effect of spindle speed on spindle temperature is apparent and nonlinear; doubling or tripling the spindle speed does not linearly affect the temperature difference. The reasons behind this nonlinearity are the friction mechanism taking place in the bearings, nonlinear nature of the heat transfer taking place in the entire spindle assembly and the convectional coefficients used in the heat distribution calculations.
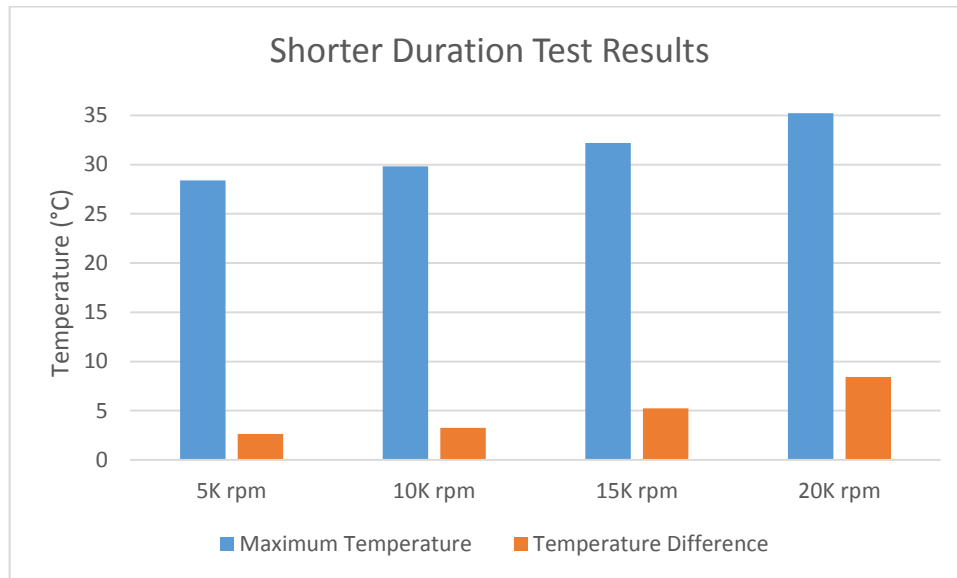
Figure 5. 12: Graph of the shorter duration test results

Deflection results of the shorter duration tests are given in Figure 5. 13 below together with the comparisons of the results with respect to spindle speeds in Figure 5. 14. The relationship between measured deflections and spindle speed is similar to temperature-spindle speed relation. Deflections of the tool tip increases with the spindle speed; but again in a highly nonlinear fashion. It is also noted that the deflection value at 20000rpm is very close to the long duration test result; so the shorter duration of 30 minutes is the settling time for the spindle deflections. From 30 minutes to 90 minutes, only 2,7 μm of deflection is added to the system. These results prove that the shorter duration tests of 30 minutes are powerful enough to represent overall spindle thermal characteristics for the investigated spindle unit. The optimal duration for the simulations can be calculated by trial and error methods for different systems, there aren't any rules regulations or rule of thumbs for this selection.
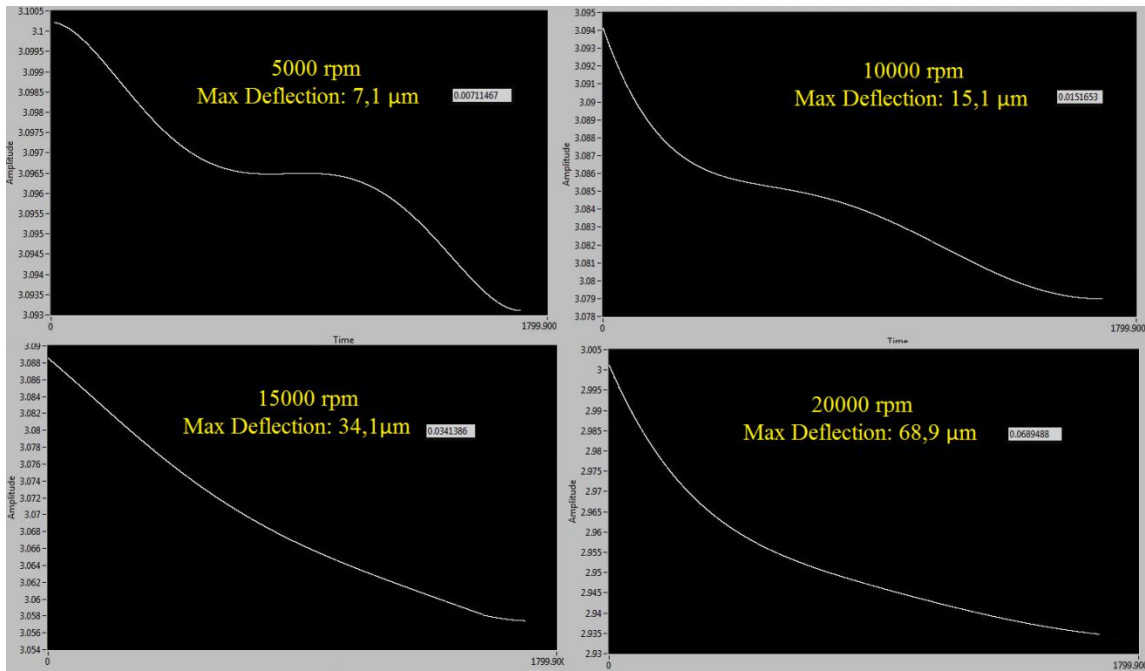
Figure 5. 13: Deflection results of the shorter duration tests
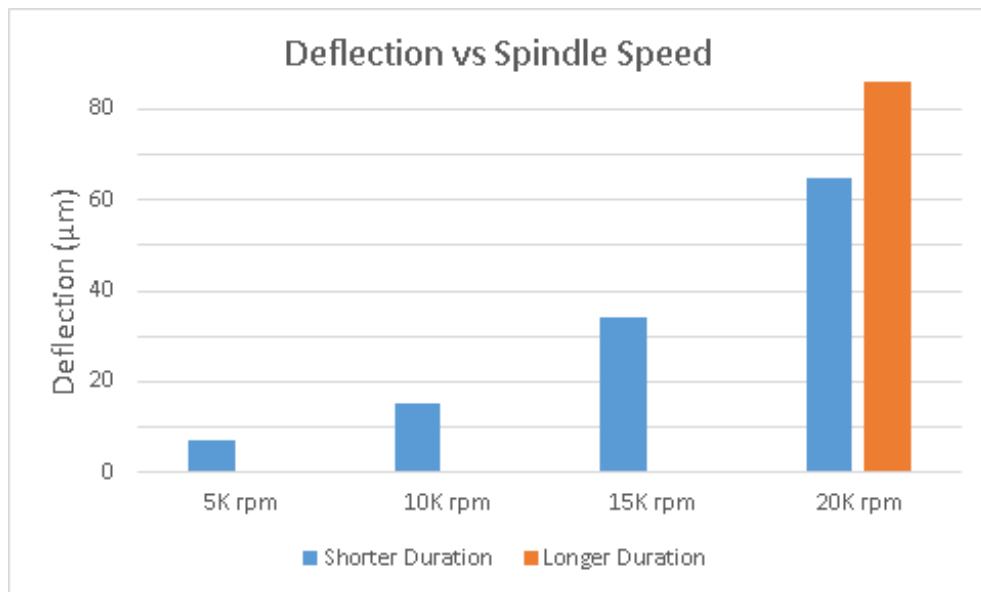
Figure 5. 14: Comparison of results according to spindle speeds

Shorter duration test results are also statistically analyzed by comparing the results of the conducted tests. Short duration tests are repeated five times for each spindle speed; on the other hand the first 30 minutes of the two long duration tests can also be considered as separate short duration tests again for each spindle speed. There are seven different test results for 5K, 10K, 15K and 20K rpm spindle speeds. The comparison of these tests are plotted and given in Figure 5. 15. According to the graph, all seven tests have generated pretty close and repetitive deflection results at the tool tip.

51
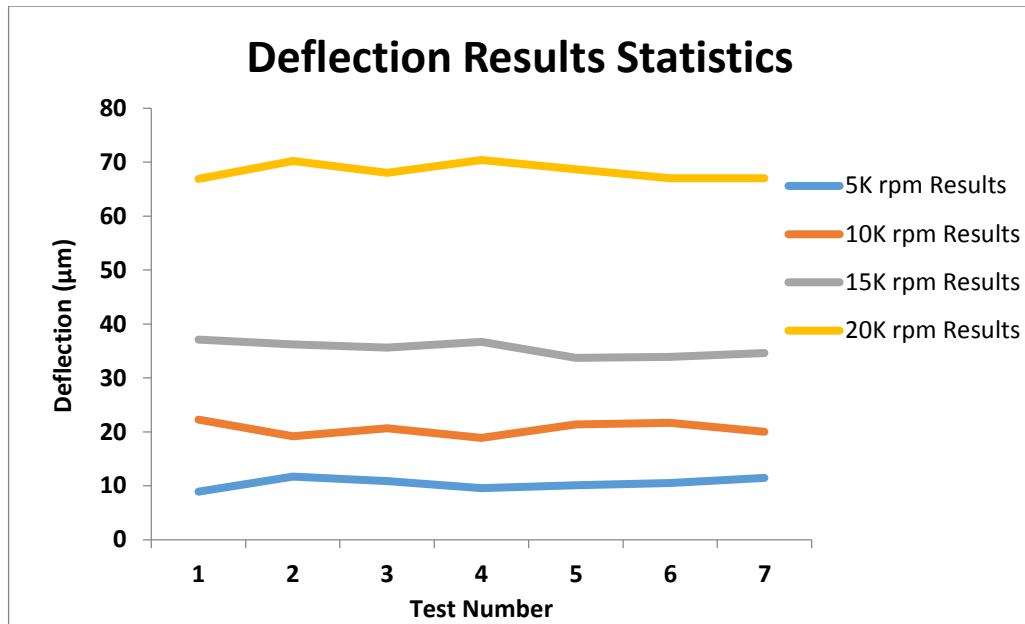
Figure 5. 15: Deflection statistics of the short duration tests

5.4 Variable Spindle Speed Test Results

Variable spindle speed tests are done according to the procedure stated in ISO 230-3 [36] under variable speed spectrum tests. Spindle speed profile stated in ISO 230-3 for variable speed tests is given in Figure 5. 16 below. Since there are lots of different machine tools with different configurations and power options used worldwide, instead of specifying numerical spindle speed values for the thermal performance tests, ISO constructed a speed profile by using percentages of the maximum allowable spindle speed of the machine tool unit which is under inspection. Maximum allowable spindle speed of the investigated 5 axis machine tool is 20,000 rpm, temperature results of the variable spindle speed tests are given in Figure 5. 17 for all 18 intervals of 15 minutes each.

Temperature plot is quiet similar to the spindle speed profile due to the direct proportion between spindle speed and heat generation of the bearings. Maximum temperatures are measured at the end of maximum spindle speed intervals, which are 2nd and 16th intervals shown with black color. Largest temperature drops are also measured in the zero spindle speed intervals, 5th and 12th intervals shown with white colors. Throughout the variable spindle speed test highest temperature recorded is at the 16th interval as 36°C while the lowest temperature is at the beginning of the test and 25°C. Maximum

52
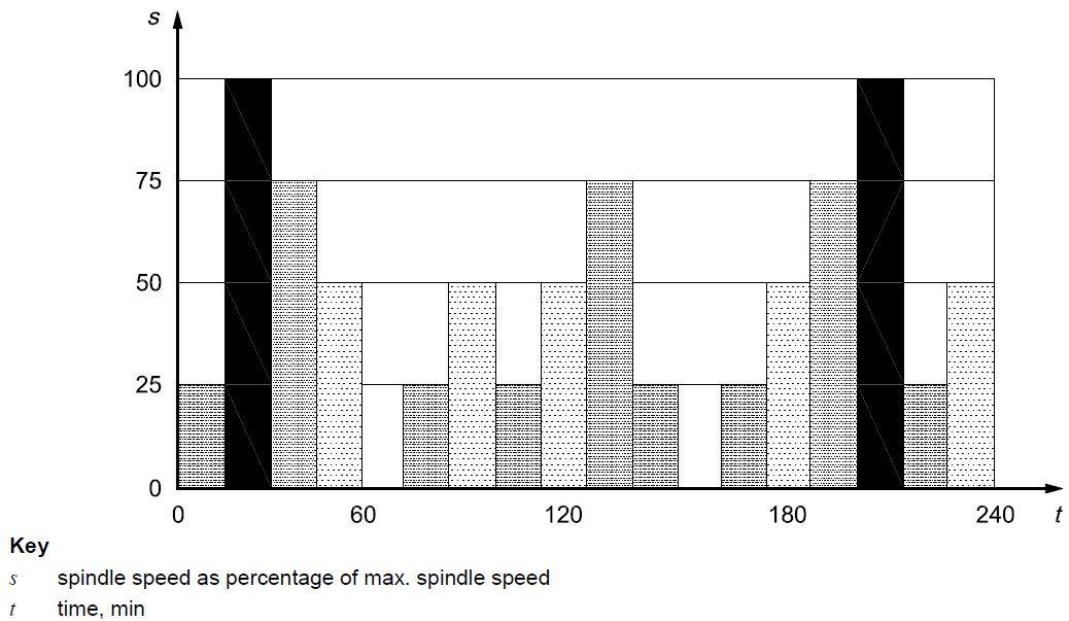
Figure 5. 16: Spindle speed profile presented in ISO 230-3

temperature difference is 11°C according to the temperature data. The reason of maximum temperature being recorded at the 16th interval apart from the direct proportion between spindle speed and heat generation is the direct proportion between the temperature rise and running time of the spindle unit. The relationship of operating time and spindle temperature is investigated by conducting tests with different durations which will be shown in the following sections.
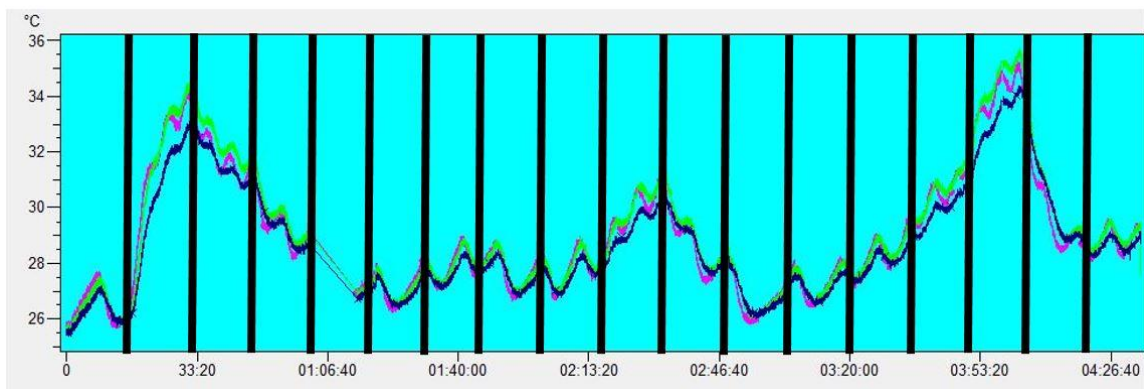
Figure 5. 17: Temperature results of the variable spindle speed tests

Displacement results of the variable spindle speed tests are given in Figure 5. 18 as filtered versions, Moving average filter formed in MATLAB is used to eliminate the effects of the measurement noise. Deflections measured in X and Y directions are 1,5

μm and 3 μm, these are negligible considered to the Z direction results; however during the 3rd, 10th and 15th intervals high amplitude oscillations are observed in these directions. The common property of all these intervals is the spindle speed, which is 15,000 rpm. The reason for these oscillations is generating a very close modal frequency to the first vibration mode of the test mandrel by rotating the spindle at 15,000 rpm; so that the vibration mode is excited. This is why the oscillations are seen only in the 15,000 rpm intervals. The maximum deflection of the tool tip is measured as 73 μm at the end of the 16th interval of Z direction, which is also the time that the maximum temperature is measured. According to the Z direction deflections it is obvious that the deflections are increasing rapidly as spindle speed reaches %75 of the maximum allowable speed or higher.
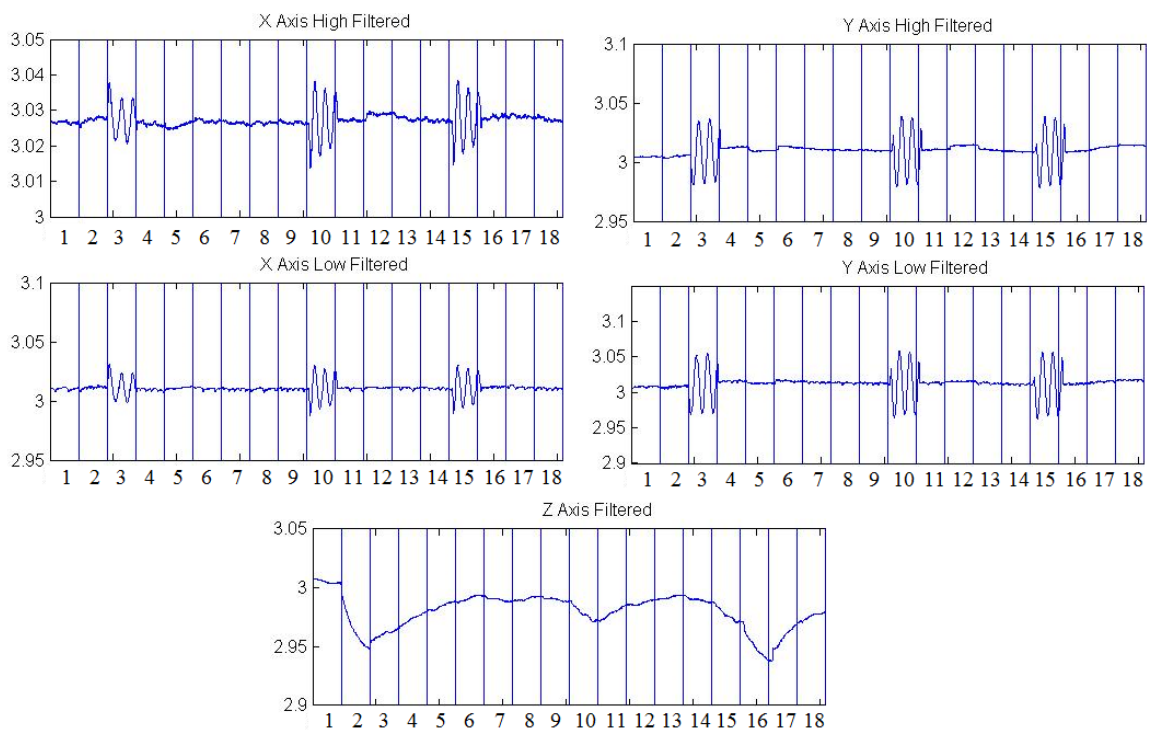
Figure 5. 18: Displacement results of the variable spindle speed tests

5.5 Comparison of Shorter Duration Constant Spindle Speed Test Results and FEM Simulations

The FEM model explained in the previous chapter is used to predict temperature distributions of the spindle unit as well as the thermally induced deflections of the tool tip. Verification process of the FEM model includes comparisons of model simulations

54

and spindle warming tests shown in the above section. Shorter duration tests are conducted for this verification purposes. The results of the FEM simulations for 5000-10000-15000 and 20000 rpm spindle speeds and 30 minutes of running time are compared to the temperature and deflection measurements of these shorter duration tests. Overall prediction accuracy of the FEM model is checked.

    a) Temperature Comparisons

Temperatures of the hottest regions for both FEM model and warm-up tests are compared and given in Figure 5. 19. The difference between the test and simulation results stars with 1,9°C for 5000 rpm and continues as 1,1 °C for 10000 rpm, 2°C for 15000 rpm and 4°C for the max speed. The maximum error is calculated in the maximum spindle speed of 20000 rpm tests. The difference is increases with the increasing spindle speed; however it can be concluded that there is a good agreement between test results and model predictions. For a highly nonlinear temperature problem having a maximum error of 4 °C with a FEM model is considerable. So the proposed FEM model can be used for predicting the temperatures of the spindle components.
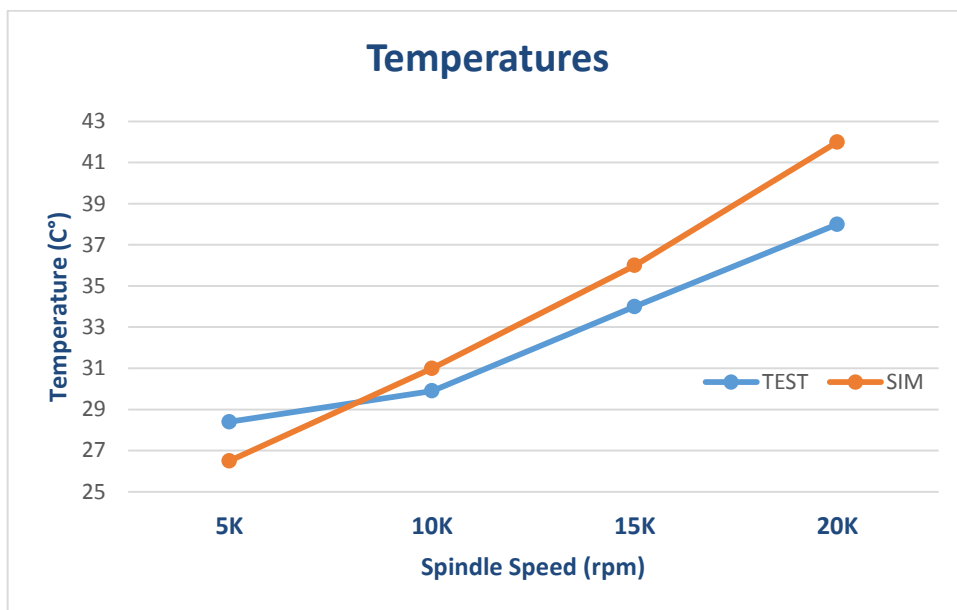
Figure 5. 19: Comparison of temperatures for experiments and simulation results

    b) Comparisons of the Tool Tip Deflections

55

Thermally induced deflections of the tool tip are measured during the experimental tests and they are also calculated with the FEM model. Comparisons of these results are shown in Figure 5. 20 for different spindle speeds. It is obvious that the FEM model is more accurate in predicting the deflections compared to the temperatures. Maximum prediction error of 5,6 µm is achieved for the 10000 rpm spindle speed tests. FEM model performs better for the higher spindle speeds, 15000 and 20000 rpm simulations. Together with the temperature comparisons, proposed FEM model is validated for predicting the tool tip deflections and temperature distributions of the spindle unit. Since the FEM model represents the thermal characteristics of the spindle system investigated, it can now be used for design optimizations and cooling system parameter selection processes without requiring real life tests and experiments.
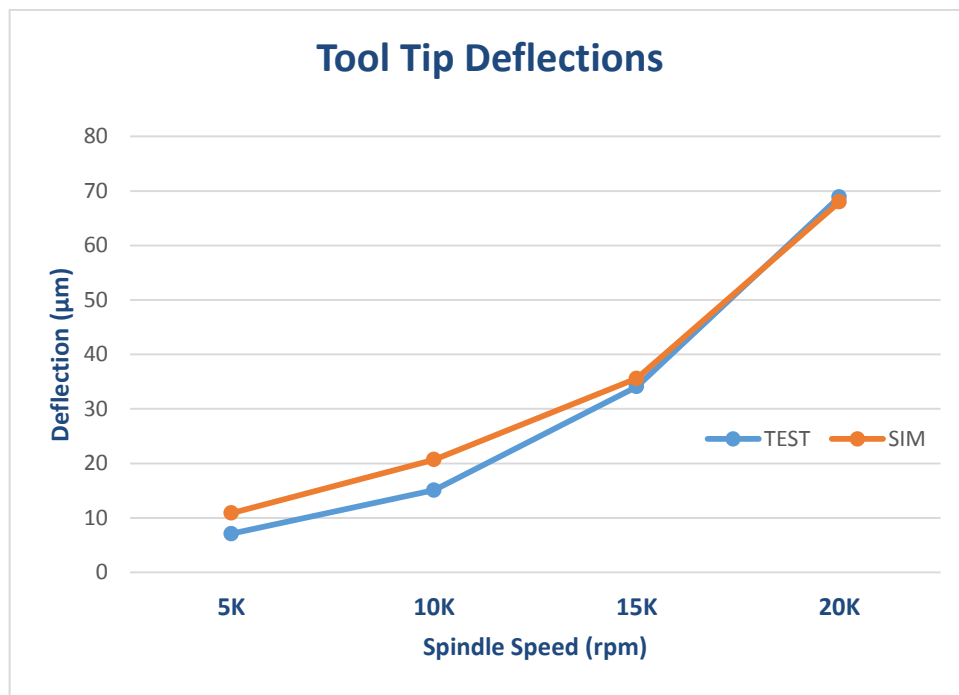
Figure 5. 20: Deflection comparisons of different spindle speeds

5.6 Identification of the Tool Tip Deflection Sources

The thermally induced deflections measured at the tool tip are basically the combination of individual spindle component deflections. The three main spindle components contributing to the tool tip deflections are the spindle shaft, column and the housing. The individual thermal deflections of these three components are generating the resultant tool tip deflection of the spindle unit; which is directly affecting the positioning accuracy of the machine tool. Identification of the individual deflections of

these parts is crucial for optimizing the overall thermal performance of the machine tool unit. In order to identify the individual thermal deflections of the spindle column housing and the shaft further experiments are conducted. These experiments are quiet similar to the previous tool tip deflection measurements; but the locations of the capacitive displacement sensors are changed to measure the three different sources. The set-up and the sensor positions of the identification tests are shown in Figure 5. 21. Two different tests are conducted for the identification of the deflection contributors; in the first test four of the displacement sensors (Disp-Sens #1,#2,#3 and #4) are positioned as shown below to measure the Z axis level of the spindle housing while the fifth sensor (Disp-Sens #5) is recording the position of the tool tip in the Z-axis. The positions of the four displacement sensors are changed to measure the Z level of the spindle column for the second test. Duration of the tests are 90 minutes and the displacement results recorded by each sensor during both tests are given in Figure 5. 22.
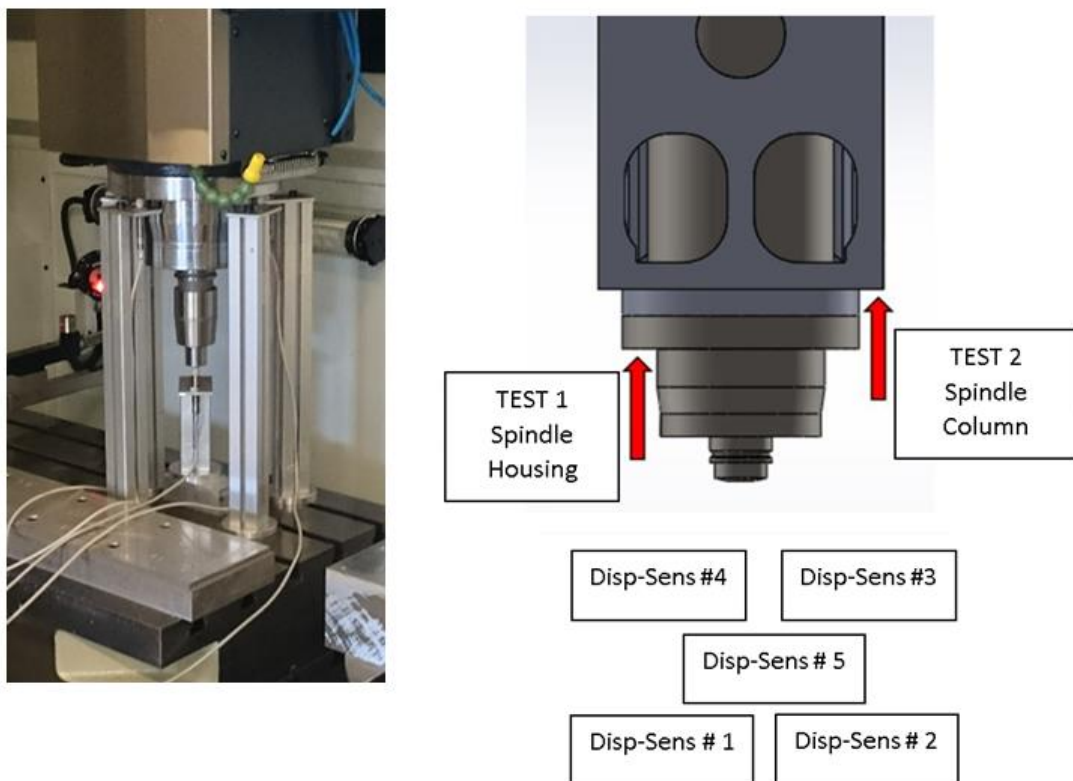
Figure 5. 21: Identification tests, set-up and displacement sensor positions
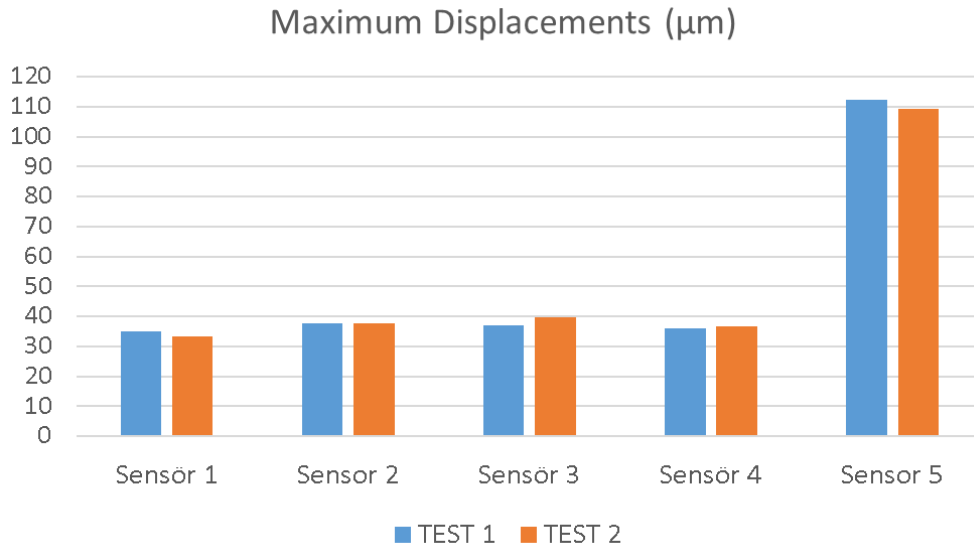
Figure 5. 22: Displacement results of the identification tests

The deflection results of the identification tests are clearly showing that there is no difference between the deflections of the spindle housing and spindle column; they are almost exactly equal to each other and responsible for the 40µm of the total deflections. Displacements sensors from #1 to #4 are showing the deflections of the housing and column in both tests, displacement sensor #5 on the other hand is showing the total deflection including the spindle column, housing and shaft. The maximum deflection value is recorded at the tool tip for both tests and it is 110µm. According to the identification tests %34 (37µm) of the total tool tip deflection is due to the thermal deflection of the spindle housing and spindle column together while the remaining %66 (73 µm) of the total tool tip deflection is due to the thermal elongation of the spindle shaft. The identification tests are also simulated by using FEM model to check the model prediction performance. The FEM simulation result for the identification case is given in Figure 5. 23. The FEM model predicts the total tool tip deflection as 97,8µm and the deflection due to the spindle housing/column as 31,6µm. There is approximately %15 difference between the test and simulation results for the identification tests; which can be considered as a good estimate for a FEM model.
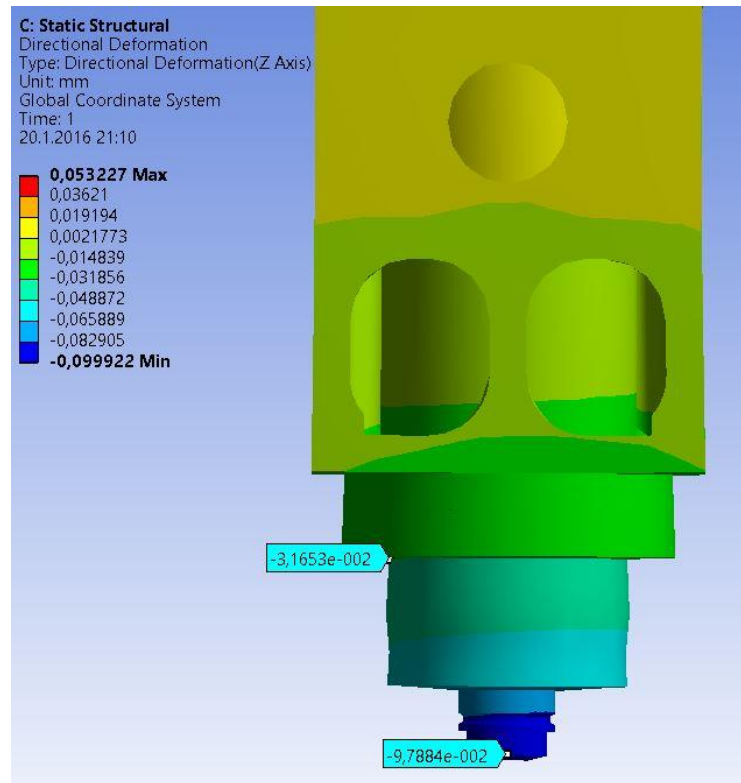
Figure 5. 23: FEM simulation result for identification tests in Z direction deflections5.7 Summary

In this chapter details of the validation tests are explained in detail together with the temperature and thermal deflection results obtained for previously defined spindle speeds. Machine tool is tested for the international standards by implementing the different procedures of the ISO, results are presented. Simulation results presented in the Chapter 4 are compared with the real test results shown in this chapter. Developed FEM model is validated for the estimation of temperature distributions and thermally induced deflections by demonstrating the good agreement between test and simulation results.

CHAPTER 6

6. COOLING SYSTEM OPTIMIZATIONS

6.1 Introduction

Cooling system is one of the most important factors affecting the thermally induced errors of the machine tool spindle systems. Heat generated by the rotating components and electrical circuits are all removed by the cooling system. Previously introduced FEM spindle thermal model is proved to be accurate in predicting the heat distributions and thermal elongations. In this chapter this FEM model is used to simulate the performance of the cooling system. Cooling system is investigated and optimized in two different steps; first step is to find optimal cooling system parameters without changing the design or components while second step is to determine the optimal cooling channel design to achieve better temperature distributions. For both steps FEM model is used and simulation results for the previously investigated cases are compared. According to the results of these simulations further design recommendations are prepared for the new, thermally stable machine tool spindle unit.

6.2 Parameter Optimizations

Cooling system performance depends not only on the components used in the system but also to the parameters used in the cooling system. It is possible to achieve better cooling performance from the same cooling unit with different and optimized

parameters. The 5 axis machine tool investigated in this study has a standard cooling system as explained in detail in the previous chapters. The problem with this cooling system is that the fluid pump used within the unit is a constant output (non-programmable) pump; so that the pressure, velocity or the flux of the cooling fluid cannot be changed. In the parameter optimization studies, FEM thermal spindle model introduced throughout this thesis is used to simulate the effects of different cooling fluid inputs; such as fluid velocity entering the cooling channels, pressure of the cooling fluid within the cooling channels or the initial temperature of the cooling fluid. By the help of these simulations optimized parameters are found and possible cooling performance improvements are predicted. The optimized cooling system parameters can be implemented to the current system by changing only the fluid pump within the cooling system.

a) Effect of Cooling Fluid Velocity

The velocity of the cooling fluid entering to the machine tool spindle is a critical factor for the overall cooling system. There are some constraints for the fluid velocity due to the power of the pump used, cooling channel geometry and efficiency. Higher fluid velocities are of course better for the cooling performance; but there are some physical limitations to that. The effect of the fluid velocity is investigated through the FEM model constructed in the study. The default value for the fluid velocity is 0.4 m/s, in order to find out the effect of the fluid velocity in both higher and lower velocity cases are simulated. Velocities chosen for these simulations are 0.08m/s, 0.8 m/s, 2 m/s and 4 m/s respectively. Simulations are conducted for the 20K rpm spindle speed case; since it has the smallest estimation error by the FEM model for the tool deflection. Comparison graph of the results are plotted and provided in Figure 6. 1 and Figure 6. 2. The effect of the cooling fluid velocity on the tool tip deflections and maximum temperatures is obvious, higher fluid velocity results in lower temperatures and less deflections at the tool tip accordingly. Increasing the velocity of the cooling fluid also increases the heat transfer coefficient. Increased heat transfer coefficient means that the same amount of cooling fluid can absorb more heat from the spindle components. This relationship is previously shown in the heat transfer coefficient calculation of the rotating shaft in Chapter 3 by equation 15. According to the graphs, it is shown that the cooling

performance can be enhanced by maximizing the cooling fluid velocity entering to the system.

Figure 6. 1: Comparison of different fluid velocities for the deflections
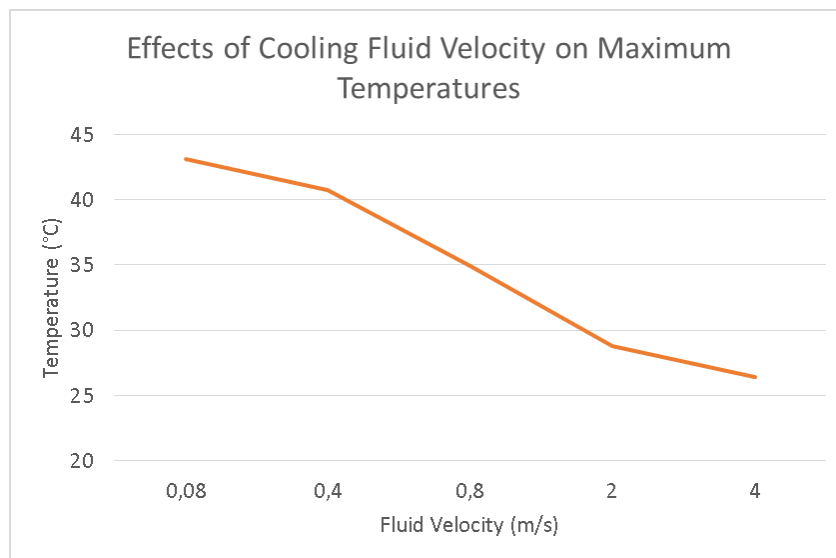
Figure 6. 2: Comparison of different fluid velocities for the temperatures

b) Effect of Cooling Fluid Temperature

Second important input to the cooling system model is the initial temperature of the cooling fluid entering to the system. This is a critical parameter for overall machine tool performance since it experienced that decreasing the initial temperature under a critical value caused instant bearing failure due to condensation taking place within the

bearings. If the initial temperature is too low, there will be a large temperature difference on the bearings causing serious condensation of vapor resulting in bearing failure. Only solution for this kind of a problem is to change entire bearing sets within the spindle assembly, which is very costly. Temperatures investigated in the simulations were selected together with the machine tool builders to utilize their experience in this issue. In the simulations, the default cooling water temperature entering to the system is 23°C; effects of temperatures 25°C -21°C -19°C -17°C were simulated through the FEM model respectively. Comparisons of the results are plotted in Figure 6. 3 and Figure 6. 4. Similar to the cooling fluid velocity, initial temperature of the cooling fluid is influencial for both tool tip deflections and maximum temperatures observed on the spindle components. The initial temperature of the cooling fluid is important for determining the temperature difference between the heat source and the heat sink. Since the only heat sink of the system is the cooling fluid, decreasing the initial temperature of the cooling fluid increases the temperature difference and heat transfer rate. Decreasing the initial temperature of the cooling fluid also lowers the thermal equilibrium point; which means observing lower temperatures at the end of the heat transfer and resulting in less tool tip deflections.

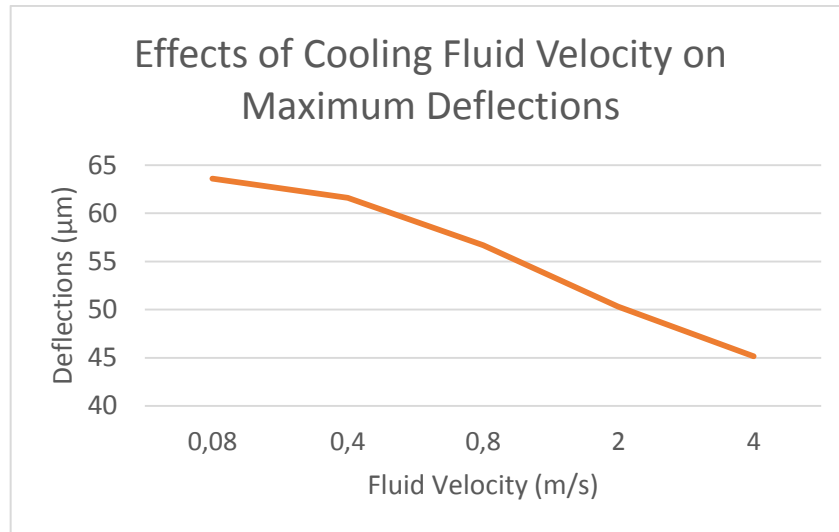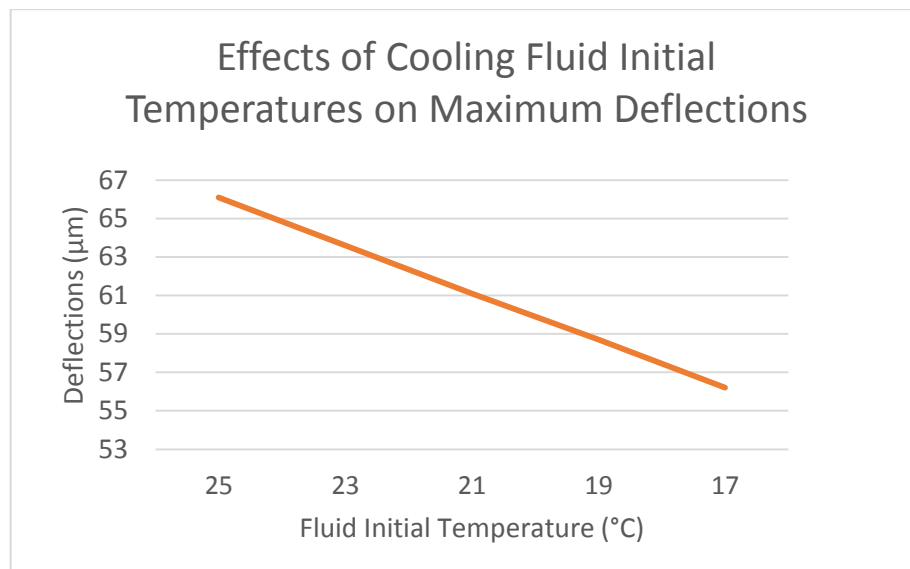Figure 6. 3: Comparison of different fluid initial temperatures for the deflections
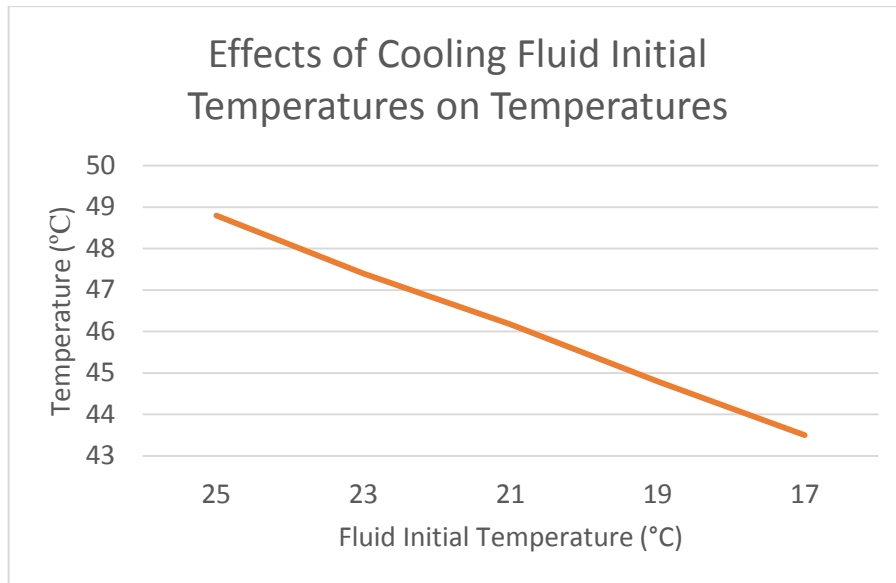
Figure 6. 4: Comparison of different fluid initial temperatures for the temperatures

6.3 Design Optimization

Cooling system performance can be improved by tuning the system parameters as shown in the above section. However there are physical limitations to the parameters that can be tuned to improve the cooling performance. For instance the velocity of the cooling fluid is limited by the power of the hydraulic pump used in the chiller unit; similarly the initial temperature of the fluid is limited by the bearing condensation problem which limits the minimum temperature of the cooling fluid at 18ºC for the investigated spindle unit.For the spindle cooling systems, design of the cooling channels are the most important factor on the overall cooling performance. For instance, relative position of these channels to the main heat sources of the spindle unit, surface areas of the channels, cross-sections of the channels, locations and amount of the channel inlets/outlets are some of the important features regarding to the cooling channel design. For the investigated machine tool spindle unit, current channel geometry is modified in the simulations considering several cooling channel designs from the literature. Some of the FEM model simulations are repeated with the new channel embedded spindle CAD models. Temperature distributions and the resulting thermal deformations are compared with the current design. According to the results of these simulations further design recommendations are outlined to be used in the completely new, thermally stable spindle design.

a) Axial Cooling Channels

Axial cooling channels are used for machine tool spindle cooling systems very often, especially for the air-spindles. Symmetric geometry of these channels provides better cooling performances than some other non-symmetrical channel designs. Cooling performance of the axial fluid channels are studied before by using FEM analysis, in these studies the convection coefficient of the axial channels are compared to the convection coefficients of other (helical) channel designs. It has been shown that axial cooling channel geometry performs better that the helical channels for the same total channel length.[37]. Axial channel geometry is created in 3D CAD model for the FEM simulations to calculate the thermal elongations and the spindle temperatures. Cross-sections of the cooling channels are kept constant (same as the original channels) in order to be able to compare the cooling performances equally. The new axial cooling channel geometry is shown in Figure 6. 5. Axial cooling channel simulations are calculated for the 20K rpm spindle speed case; because 20K rpm simulation is the case which FEM model has the smallest estimation error compared to the test results. Results of the axial cooling channel geometry are shown in Figure 6. 7. Deflections calculated for the axial cooling channels are also shown in Figure 6. 6 . There are two separate temperature fluctuating regions observed in each simulation results; these regions are the closest parts of the cooling channels to the upper and lower bearings. Higher temperatures are observed at the lowest part of the axial cooling channels; similar to the default channel geometry simulation results; because the most powerful heat source of the spindle unit, lower bearings, are located exactly near to it. The comparison of the deflection results for the axial and default channel geometries clearly show that the axial channels are performing better in every spindle speed. A possible reason for axial channels to perform better than the default channel design is the total length of the cooling channels. Axial channel design can fit longer channels to the same spindle body compared to the default design; the axial channels are % 15 longer, in total, than the default channels.
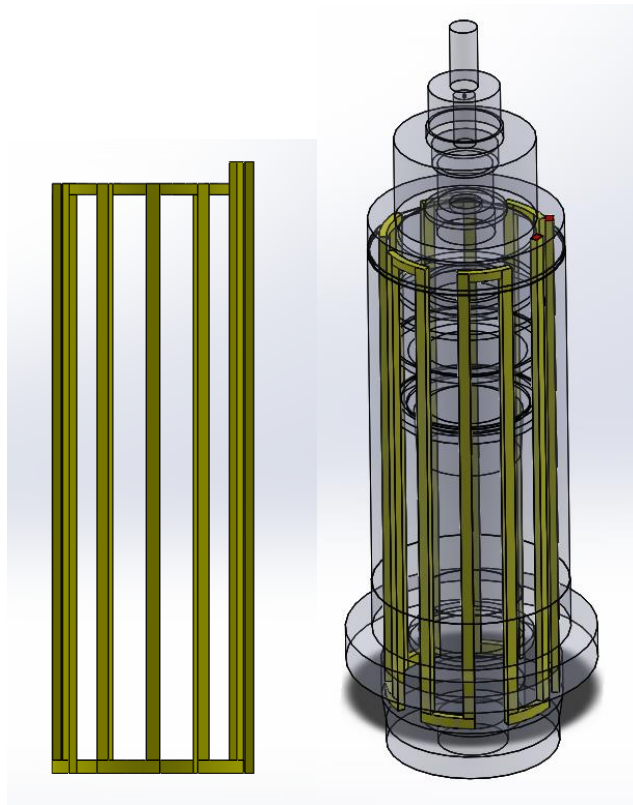
Figure 6. 5: Axial cooling channels
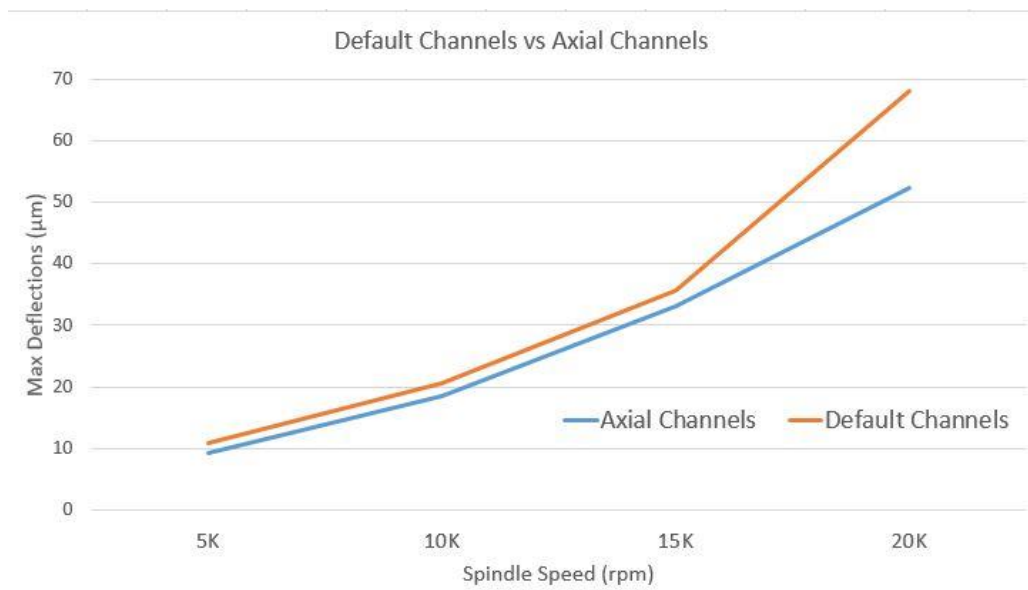
Figure 6. 6: Comparison of default cooling channels with axial cooling channels
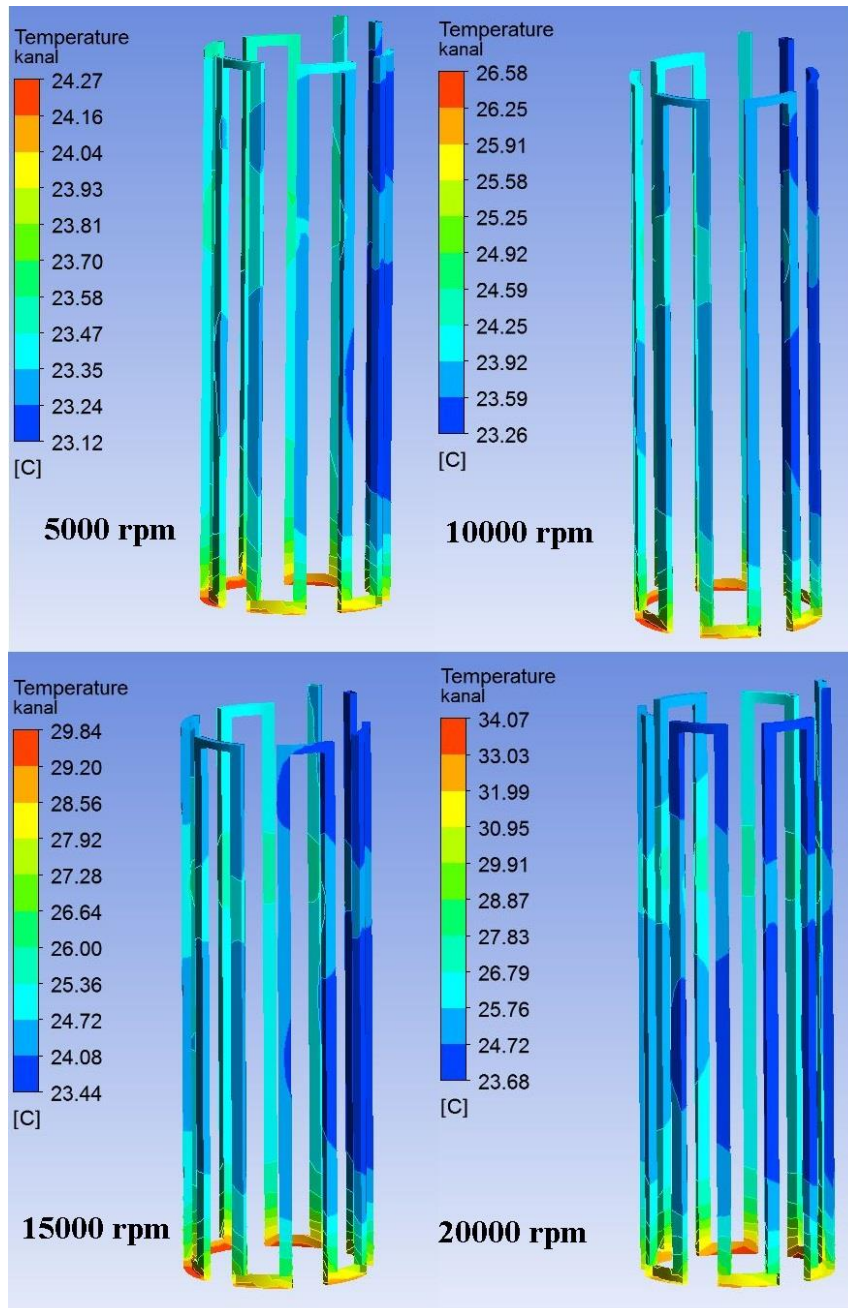
Figure 6. 7: Temperature distribution of the axial cooling channels

b) Cooling Channels with Lower Helix Angle and Unified Diameter

Helix angle is an important parameter of the helical cooling channels affecting the cooling performance. Number of rows change according to the helix angle for channels with fixed heights. Increasing the helix angle will result in less number of rows so that it will directly result in worse cooling performances. In order to optimize the cooling performance, simulations are conducted only for the lower helix angle case instead of higher angles .The helix angle used in the simulation is 7,45° while the default helix

angle of the cooling channels is 9°. Helix angle depends on the overall geometry of the spindle unit such that it is impossible to make drastic changes. Default channel geometry is modified by using lower helix angles and unifying the overall channel design. Symmetricity of the entire cooling channel geometry is also achieved by the newly designed geometry. The new solid model of the proposed channel geometry is created in FEM to calculate temperature distributions and thermal deformations accordingly. The new cooling channel geometry with lower helix angle is illustrated in Figure 6. 8. Results of the new channel geometry are shown in Figure 6. 10 and Figure 6. 10. By lowering the helix angle, the total length of the cooling channels is increased by a small amount; but unifying the channel diameters along the spindle column reduced the effect of the increment in the total length. In the end performances of the default channel design and the unified-lower helix angle channel design are compared with respect to the amount of deflection they generated. It is shown that there is no significant difference between their performances; default channels are performing better in the so called lower spindle speeds while the new design generates less deflections at the higher spindle speed cases.
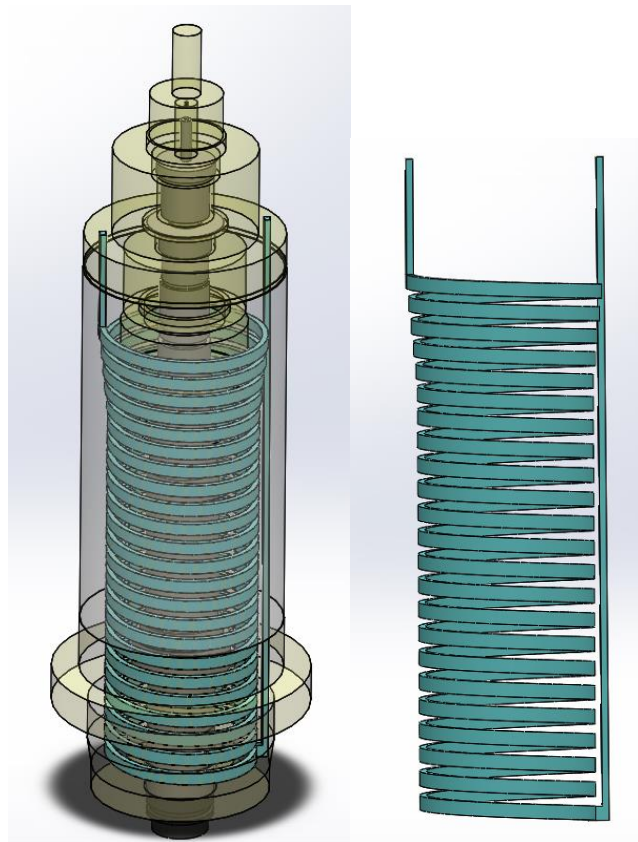
Figure 6. 8: Lower helix cooling channel geometry
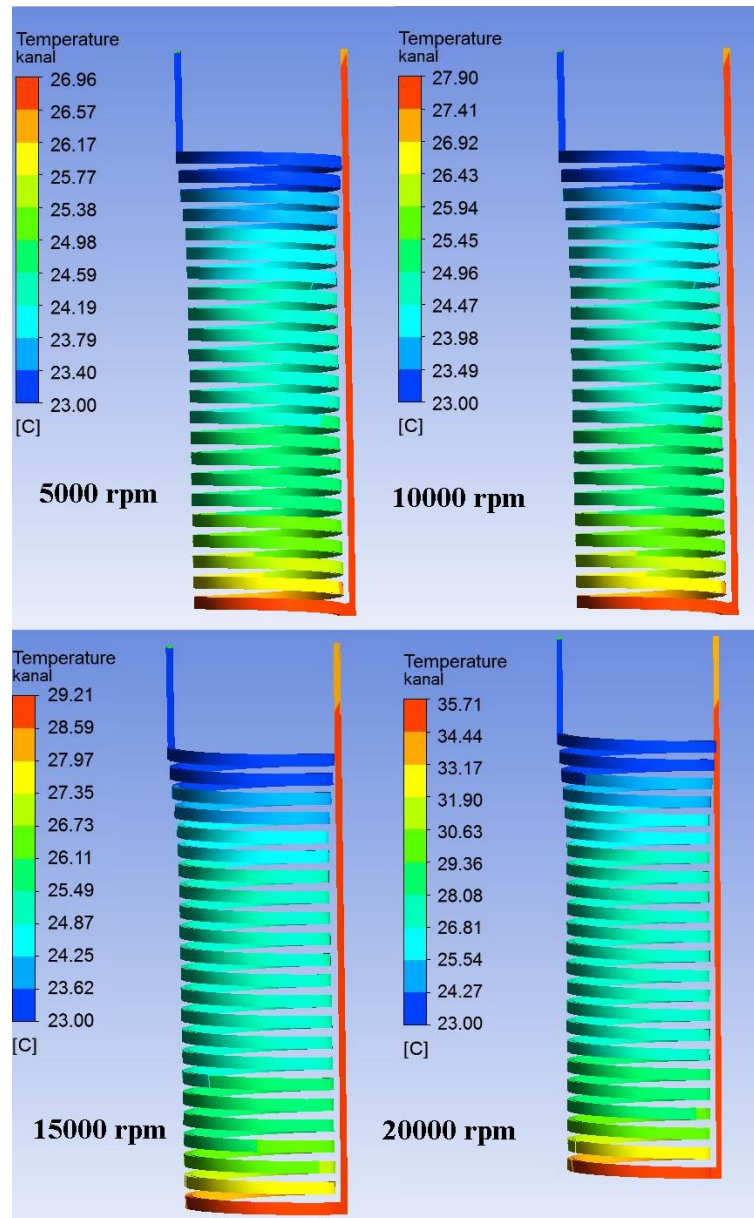
Figure 6. 9: Lower- unified helix simulation results

6.4 Summary

In this chapter, FEM model developed in the previous sections is used to optimize some of the input parameters of the system. Number of the parameters to be optimized is very limited due to the conservative design of the cooling system. Only the effects of initial fluid temperature entering to the system and the fluid velocity are investigated in the FEM simulations. It is shown that the both parameters are playing an important role on the spindle unit temperature distribution and tool tip deflections. Lowering the initial temperature of the cooling fluid together with increasing the velocity of the cooling

fluid entering to the cooling channels will directly improve the thermal performance of the investigated spindle unit. It also underlined that the optimization of these parameters are limited due to the physical constraints of the cooling system and spindle unit components; for instance the power of the fluid pump for the velocity and the water
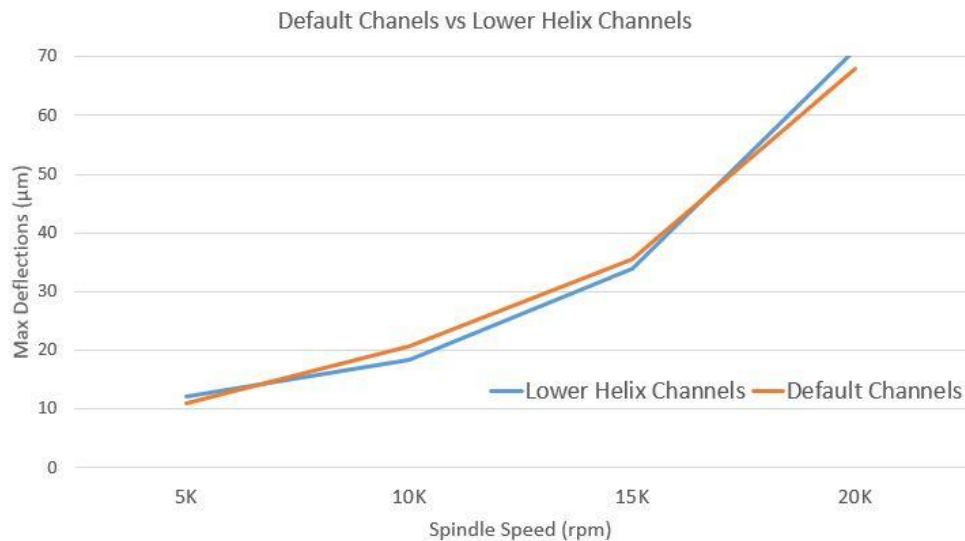
Figure 6. 10: Comparison of default cooling channels with lower helix cooling channels

condensation problem of the spindle bearings for the initial fluid temperature. For the design optimizations section, two new designs are constructed and tested via the FEM model. Results of these new designs are compared to the default systems results. It is shown that the axial cooling channels perform better than the default design while lowering the helix angle and unifying the diameter of the cooling channels along the spindle unit does not have an important effect on the cooling performance. The effect of the total cooling channel length is an important reason for axial channels to perform better, the %15 difference in the total cooling channel length resulted in average of 1,3 ºC lower temperatures for the axial channels when compared to the lower-unified helix angle channels in all four different spindle speeds.

CHAPTER 7

7. SUGGESTIONS FOR FURTHER RESEARCH

Thermal aspects of a 5 axis vertical machine tool spindle unit are analyzed by the constructed FEM model throughout the study. The performance of the FEM model is validated by the measurements; however there are still some points of improvement for the study. Following recommendations may improve the presented model in the means of prediction accuracy, robustness and calculation times:

- Heat sources used in the presented FEM model can be extended by including the heat generated by the motor, heat generated by the moving axes and heat generated in the ball-screws in order to represent all of the possible heat sources in a machine tool. The only heat source used in the presented model is the heat generated by the spindle bearings; due to the fact that the most of the heat generated in the machine tool is generated by the spindle bearings. Adding other heat sources may increase the model complexity and calculation times.

- The effect of the additional cooling systems, such as through coolant may be included to the model to see if there is a drastic improvement in the thermal behavior of the machine tool.

- Optimizations presented in this study are only based on the current spindle design (cooling channel cross sections are kept constant, location of the channels are kept constant…etc.); however completely new channel designs may be simulated for increasing the thermal performance of the machine tool.

- Parameter optimizations are also limited by the physical properties of the current cooling system. The only parameters that can be tuned are used for optimization

purposes; but the number of parameters that can be tuned may be increased by changing the physical properties of the cooling system. Simulations may be extended to see the amount of improvement for changing the cooling unit with a new, more powerful and adjustable cooling unit.

- The effect of the material properties of the spindle unit components are not investigated in this study; however it is know that the thermal behavior is highly depending on the material properties. Simulations may be extended by considering different material for the spindle unit components. System optimization may be achieved by better material selection.

CHAPTER 8

8. DISCUSSIONS AND CONCLUSIONS

High speed spindle units are inseparable components of the current machine tools used in precision machining industries. Demand for tighter tolerances together with lower scrap ratios and minimal costs are increasing rapidly as the technology develops. In order to satisfy these demands, manufacturing industry needs faster, more accurate and more efficient machine tools. Main aim of this thesis was to develop a practical tool for machine tool users to estimate thermal performance of the machine tools easily. Conclusions and the contributions of the thesis are as following:

- It is shown that the heat generated at the angular contact bearings is directly proportional to the applied loads and the spindle speed; but there is no linear trend between these parameters and the temperature distributions.
- The importance of bearing selection, deciding the bearing diameter and the amount of the preload that is going to be applied on these bearings, is emphasized by showing the effects of both bearing diameters and the preloads on the generated bearing heat.
- It is shown that the accurate prediction of the machine tool spindle temperature distributions can be achieved by modelling the most important heat sources within the spindle assembly, spindle bearings.
- The relationship between the temperature distribution and the thermally induced errors are underlined by the conducted experiments and FEM simulations; so

that by reducing both the maximum temperature value and its accumulation near to the tool tip, thermal performance can be enhanced.

- The velocity and the initial temperature of the cooling fluid used in the cooling system are influential on the final thermally induced errors and these parameters are needed to be tuned.

- Performance of the cooling system can be enhanced by simply changing the channel geometry, without changing the cross-sections or the flow rate.

- Developed FEM model in this study is a generic model which can be used with any other spindle and cooling system designs by simply uploading the 3D CAD model of the new spindle unit to be tested. This feature enables machine tool builders, Spinner Machine Tools in the context of this study, to simulate their prototype designs for better cooling performances.

- By using the developed FEM model both design and parameter optimizations can be done for the machine tools. External parameters of the cooling system such as the power of the fluid pump, pressure of the cooling fluid or the set temperature of the cooling fluid can be tuned by conducting several simulations. Spindle design on the other hand can also be optimized by simulating the temperature distributions and the thermal deformations of various possible designs as shown by simulating axial and lower helixed cooling channel designs in chapter 6.

REFERENCES

[1]   Bryan, J. International status of thermal error research. (keynote) CIRP Annals 16, (1968)

[2]   Bryan, J., Pearson, J., Machine tool metrology. ASTME Conf. Sun Francisco, UCRL 71164 (1968)

[3]   Bryan, J., Clouser, R., and McClure, E.. Expansion of a cutting tool during chip removal. CIRP Annals 16, (1968)

[4]   Bryan, J., Donaldson, R., Clouser, R., Blewett W., Reduction of machine tool spindle growth. NAMRC, McMasters Univ. UCRL 74672 (1973)

[5] Sata, T., Takeuchi, Y., Sakamoto, M., & Weck, M. (1981). Improvement of working accuracy on NC lathe by compensation for the thermal expansion of tool. CIRP Annals-Manufacturing Technology, 30(1), 445-449.

[6] Weck, M., et al. "Reduction and compensation of thermal errors in machine tools." CIRP Annals-Manufacturing Technology 44.2 (1995): 589-598.

[7] Wang, Y., Zhang, G., Moon, K. S., & Sutherland, J. W. (1998). Compensation for the thermal error of a multi-axis machining center. Journal of materials processing technology, 75(1), 45-53.

[8] Mou, J., M. A. Donmez, and S. Cetinkunt. "An adaptive error correction method using feature-based analysis techniques for machine performance improvement, Part 1: Theory derivation." Journal of Manufacturing Science and Engineering 117.4 (1995): 584-590.

[9] Moriwaki, Toshimichi, and Eiji Shamoto. "Analysis of thermal deformation of an ultraprecision air spindle system." CIRP Annals-Manufacturing Technology 47.1 (1998): 315-319.

[10]   Haitao, Zhao, Yang Jianguo, and Shen Jinhua. "Simulation of thermal behavior of a CNC machine tool spindle." International Journal of Machine Tools and Manufacture 47.6 (2007): 1003-1010.

[11]   Chen, Shao-Hsien, Chin-Mou Hsu, and Yi-Lang Tsai. "Measurement Technique of Thermal Temperature Rise of Double Column Machining Center." International Journal of Engineering and Industries 5.1 (2014): 48.

[12]   Wang, Yung-Cheng, Ming-che Kao, and Chung-Ping Chang. "Investigation on the spindle thermal displacement and its compensation of precision cutter grinders." Measurement 44.6 (2011): 1183-1187.

[13]   Li, Shuhe, Yiqun Zhang, and Guoxiong Zhang. "A study of pre-compensation for thermal errors of NC machine tools." International Journal of Machine Tools and Manufacture 37.12 (1997): 1715-1719.

[14]   Hattori, M., et al. "Estimation of thermal-deformation in machine tools using neural network technique." Journal of materials processing technology 56.1 (1996): 765-772.

[15]   Vanherck, Paul, J. Dehaes, and Marnix Nuttin. "Compensation of thermal deformations in machine tools with neural nets." Computers in industry 33.1 (1997): 119-125.

[16]   Mize, Christopher D., and John C. Ziegert. "Neural network thermal error compensation of a machining center." Precision Engineering 24.4 (2000): 338-346.

[17]   Palmgren, A., 1959, Ball and Roller Bearing Engineering, S. H. Burbank, Philadelphia,   PA.

[18]   Harris, T. A., and M. H. Mindel. "Rolling element bearing dynamics." Wear 23.3 (1973): 311-337.

[19]   Burton, R. A., and H. E. Staph. "Thermally activated seizure of angular contact bearings." ASLE transactions 10.4 (1967): 408-417.

[20]   Jorgensen, Bert Ray. "Robust modeling of high-speed spindle-bearing dynamics under operating conditions." (1996).

[21]   Stein, J. L., and Tu, J. F., 1994, ''A State-Space Model for Monitoring Thermally-Induced Preload in Anti-Friction Spindle Bearings of High-Speed Machine Tools,''ASME J. Dyn. Syst., Meas., Control, Sept., pp. 372–386.

[22]   B. Bossmanns, J.F. Tu, A power flow model for high speed motorized spindles-heat generation characterization, Transactions of the ASME, Journal of Manufacturing Science and Engineering 123 (2001) 494–505.

[23]   B. Bossmanns, J.F. Tu, A thermal model for high speed motorized spindles, International Journal of Machine Tools & Manufacture 39 (1999) 1345–1366.

[24]   Li, Hongqi, and Yung C. Shin. "Analysis of bearing configuration effects on high speed spindles using an integrated dynamic thermo-mechanical spindle model." International Journal of Machine Tools and Manufacture 44.4 (2004): 347-364.

[25]   Li, Hongqi, and Yung C. Shin. "Integrated dynamic thermo-mechanical modeling of high speed spindles, part 1: model development." Journal of Manufacturing Science and Engineering 126.1 (2004): 148-158.

[26]   Li, Hongqi, and Yung C. Shin. "Integrated dynamic thermo-mechanical modeling of high speed spindles, part 2: solution procedure and validations." Journal of manufacturing science and engineering 126.1 (2004): 159-168.

[27]   Min, Xu, Jiang Shuyun, and Cai Ying. "An improved thermal model for machine tool bearings." International Journal of Machine Tools and Manufacture 47.1 (2007): 53-62.

[28]   Jin, Chao, Bo Wu, and Youmin Hu. "Heat generation modeling of ball bearing based on internal load distribution." Tribology International 45.1 (2012): 8-15.

[29]   SKF Group, "Super-precision angular contact ball bearings: High-speed, B design, sealed as standard", Product Catalogue, 2102.

[30]   SCHAEFFLER GROUP, "FAG Super Precision Bearings" Issue AC4/130/7EA, Apr.2008.

[31]   Jeng, Yeau-Ren, and Pay-Yau Huang. "Predictions of temperature rise for ball bearings." Tribology transactions 46.1 (2003): 49-56.

[32]   Ashby, M. F., J. Abulawi, and H. S. Kong. "Temperature maps for frictional heating in dry sliding." Tribology Transactions 34.4 (1991): 577-587.

[33]   F.P. Incropera, D.P. De Witt, Fundamentals of heat and mass transfer, 4th Ed., John Wiley and Sons, 1996.

[34]   FRIEDHELM LOH GROUP, "Catalogue 33 Edition 2011/2012", RITTAL GmbH & Co. KG, 2011

[35]   ISO 10791-10: 2007, Test conditions for machining centres — Part 10: Evaluation of thermal distorsions

[36]   ISO 230-3:2007, Test code for machine tools -Part 3: Determination of thermal effects

[37]   MadhanMuthuGanesh, K., et al. "CFD Analysis of cooling channels in built-in motorized high speed spindle."

[38]   Yalcin,T.K, Avcı A, M.S, Budak E., "An Experimental Study for Tool Center Point Displacements of a 5-axis CNC Machine Tool due to Thermal Effects", 8th Diemold Conference, 2015

[39]   Yalcin,T.K,Erberdi M.S, Özlü E., Budak E., " Thermal Modeling of High Speed Spindles", 6th National Machining Symposium (UTIS), 2015